Dissecting neuron-specific functions of circadian genes using modified cell-specific CRISPR approaches.

Shlesha Richhariya[1], Daniel Shin[1], Jasmine Quynh Le[1] and Michael Rosbash[1*]

Howard Hughes Medical Institute, Brandeis University, Waltham, MA 02454

*Correspondence – rosbash@brandeis.edu

Preprint: Biorxiv (https://www.biorxiv.org/content/10.1101/2023.02.23.529279v1)

Classification

Major: Biological Sciences

Minor: Neuroscience/Genetics

Keywords: adult-specific CRISPR, cell type-specific CRISPR, circadian, clock neurons, vrille, cryptochrome, Pdf

Abstract

Circadian behavioral rhythms in *Drosophila melanogaster* are regulated by about 75 pairs of brain neurons. They all express the core clock genes but have distinct functions and gene expression profiles. To understand the importance of these distinct molecular programs, neuron-specific gene manipulations are essential. Although RNAi based methods are standard to manipulate gene expression in a cell-specific manner, they are often ineffective, especially in assays involving smaller numbers of neurons or weaker Gal4 drivers. We and others recently exploited a neuron-specific CRISPR-based method to mutagenize genes within circadian neurons. Here we further explore this approach to mutagenize three well-studied clock genes: the transcription factor gene *vrille,* the photoreceptor gene *Cryptochrome* (*cry*) and the neuropeptide gene *Pdf*. The CRISPR-based strategy not only reproduced their known phenotypes but also assigned *cry* function for different light mediated phenotypes to discrete, different subsets of clock neurons. We further tested two recently published methods for temporal regulation in adult neurons, inducible Cas9 and auxin-inducible gene expression system (AGES). The results were not identical, but both approaches successfully showed that the adult-specific knockout of the neuropeptide *Pdf* reproduces the canonical loss-of-function mutant phenotypes. In summary, a CRISPR-based strategy is a highly effective, reliable, and general method to temporally manipulate gene function in specific adult neurons.

47

48 **Significance statement**

49 Most animals have specific brain neurons that regulate sleep-wake cycles and other aspects of
50 circadian behavior. *Drosophila* has only about 150 of these clock neurons. Despite their small
51 numbers, they have remarkably diverse anatomy and gene expression profiles. To address the
52 different functions of these neurons, we used highly specific and efficient CRISPR-based methods
53 to create cell type-specific disruptions of three traditional circadian genes. We were able to assign
54 the function of the photoreceptor cryptochrome to two tiny subsets of clock neurons. In addition,
55 two independent methods assigned the neuropeptide PDF to the adult stage. In summary, we find
56 that the CRISPR-based methods are very efficient at studying adult specific functions of genes in
57 small, discrete sets of neurons.

58

59 **Introduction**

60 Organismal behavior involves sensing the environment, internal processing, and motor actions. In
61 multicellular organisms, this process is regulated largely by cells of the nervous system which
62 often have defined roles as parts of bigger networks and circuits. One behavior that is almost
63 ubiquitous to organisms on earth is aligning activity bouts to the daily rotations of the earth. The
64 underlying mechanism is circadian rhythmicity.

65 In *Drosophila*, circadian clocks tick away in about 75 pairs of central brain clock neurons.
66 These neurons all express the core circadian machinery, which includes the transcription factors
67 CLOCK/CYCLE and the circadian inhibitory proteins PER/TIM. Rhythmic expression of these
68 genes is important for maintaining circadian rhythmicity, and together they form a core
69 transcription-translation feedback loop whose activity can be entrained by environmental cues such
70 as light (1–3). Clock neurons also express several other proteins, such as the transcription factors
71 VRILLE (VRI) and PDP1; their rhythmic expression is important for circadian behavior (4, 5).

72 Many additional genes are specifically expressed within clock neurons and also contribute
73 to rhythmic behavior. Pigment dispersing factor (*Pdf*) encodes a circadian neuropeptide expressed
74 exclusively within the small and large LNvs; *Pdf* mutants are arrhythmic and show increased sleep
75 (6, 7). Another gene expressed by roughly half the clock neurons coding for the photoreceptor
76 cryptochrome is *cry* (8–11). Wild-type flies are arrhythmic in constant light, whereas *cry* mutants
77 are rhythmic in this condition (12). Despite the specificity in expression and probably function,
78 few studies have explored the cell type-specific functions of these genes (13), and the cellular focus
79 of many of circadian genes remains unknown.

80 Functional roles of specific circadian neurons have been broadly associated with the 7-8
81 subgroups based on anatomical location. For example, the PDF positive small LNvs are key

82 regulators of rhythmicity under constant darkness and regulate morning activity. Another group of
83 neurons, the 6 LNds along with the 5th sLNv, regulate evening activity and thus were labelled
84 evening cells (14–17). Yet other clock neuron subgroups play accessory roles in regulating
85 rhythmicity and even sleep. They include the PDF-positive large LNvs, the DN1s, the DN2s, the
86 LPNs and the mysterious DN3s (18–22)

87 Recent single cell sequencing indicates at least 17 distinct subgroups, about twice as many
88 as originally identified based on anatomical location (23). It is likely that many of these new
89 subgroups are also functionally distinct. Fortunately, many of them can now be accessed through
90 judicious use of the Gal4/UAS system (24, 25), which allows for cell type-specific perturbations.
91 This is because there are multiple Gal4 and split Gal4 drivers available to access specific circadian
92 neurons (26, 27).

93 These drivers can be combined with the standard method of UAS-RNA interference
94 (RNAi) to knockdown gene expression. Although this approach works well in many cases and has
95 been invaluable for cell type-specific perturbations, it is often variable and usually induces partial
96 knockdown (28, 29). Fortunately, it is now possible to disrupt genes completely and in the same
97 cell-specific manner using CRISPR-Cas9-based gene editing (30, 31). Cas9 is an enzyme that
98 induces a double stranded break at a specific genomic location determined by the guideRNA
99 (gRNA) sequence (32). The error prone repair machinery endogenous to all cells usually leads to
100 mutations known as indels (insertions-deletions). These range from a missense mutation to a small
101 addition or deletion causing frameshift mutations, often disrupting protein function (31).

102 Earlier adaptations of this method achieved cell specificity by expressing the Cas9 protein
103 in a Gal4 dependent manner while ubiquitously expressing a single guide RNA against a gene of
104 interest. The method was found to be more consistent and effective than RNAi in inducing loss of

105 function phenotypes (29, 33). More recent developments such as multiplexing guides against a
106 gene in an array under UAS control further improved both the efficiency and cell type-specificity
107 (33, 34). This improved method worked well for disrupting the functions of the core clock genes
108 *period* (*per*) and *timeless* (*tim*) in circadian neurons (35, 36) and it was more recently extended to
109 the disruption of genes encoding G-protein coupled receptors in these neurons (37).

110 Here, we implement this method to further understand the roles of three circadian behavior-
111 associated genes: *vri, cry* and *Pdf*. We chose to generate a CRISPR-based line against *vri* because
112 there are no successful RNAi data in the literature, and we chose *cry* and *Pdf* to address precise
113 cell type-specific functions. Lastly, the CRISPR/Cas9 strategy was combined with two recent
114 methods for temporal regulation, which successfully restricted gene editing and the resulting
115 phenotype to specific neurons in just the adult stage. The results taken together substantially add
116 to previous circadian analyses and identify specific subsets of clock neurons within which these
117 genes function to regulate behavior.
118
119

120 **Results**

121 **CRISPR mediated loss of VRI from clock neurons leads to a short circadian period.**

122 Circadian behavioral rhythms are primarily regulated by a molecular program operating in clock
123 neurons. One component of this program is the transcription factor VRI encoded by the essential
124 gene *vrille (vri)*. Homozygous mutants are developmentally lethal (38), and hemizygous mutants
125 are strongly rhythmic but with a shorter free-running circadian period (4). Cycling of VRI in clock
126 neurons is likely important as constant over-expression in clock-expressing cells causes
127 arrhythmicity and a longer circadian period (4). However, an RNAi against *vri* in clock neurons
128 did not affect circadian behavior (39). We therefore developed a line with CRISPR/Cas9 based
129 3X-guide-RNAs targeting the *vri* gene under UAS-control (*UAS-vri-g*). When expressed along
130 with the reduced expression *UAS-Cas9.P2* (29) in clock neurons and the *CLK856-Gal4* driver,
131 there was potent cell type-specific loss of VRI-staining (Fig. 1A, B, S1A). Importantly, the effect
132 was shown to be specific as only VRI levels in Gal4-labeled cells were impacted; VRI levels in
133 the DN3 neurons were unaffected (Fig. S1A) as expected since most of them are not labeled by
134 the *CLK856-Gal4* driver (23). These flies had normal behavior under 12h light: 12h dark (LD)
135 conditions, but with a small evening peak advance compared to the control strains (Fig. S1B, C).
136 Consistent with this phenotype, the flies were completely rhythmic in DD but with a significantly
137 shorter circadian period (Fig. 1C-G). These phenotypes are identical to those of a recent *vri* mutant
138 (40) indicating that they derive from the clock neurons.

139

140 **CRY functions independently in two subsets of clock neurons**

141 We next addressed the circadian gene *cry,* which encodes the photoreceptor Cryptochrome (CRY).
142 Wild type flies are arrhythmic under constant bright light conditions, *cry* mutants in contrast

143 remain rhythmic in constant light (12). This classic phenotype is reproduced when *cry* was mutated
144 with *UAS-Cas9.P2* and 3X-gRNA against cry (*UAS-cry-g)* specifically in clock neurons using the
145 *CLK856-Gal4* driver, which also led to loss of nearly all CRY staining from all clock neurons (Fig.
146 S3). Whereas only about 10 percent of the control flies were rhythmic in constant light
147 (Rhythmicity Index>0.25), 90 percent of the *cry*-mutated flies were rhythmic (Fig. 2A-C, G, Table
148 S1). These flies were also rhythmic in constant darkness, like the controls (Fig. S2) and like
149 traditional *cry* mutants (12).

150 As *CLK856-Gal4* is expressed in most clock neurons, we then asked if the constant light
151 phenotype could be assigned to a more specific subset of circadian neurons. CRISPR-mediated
152 cell type-specific mutagenesis of *cry* led to loss of CRY staining from specific neurons (Fig. S3).
153 All PDF neurons are CRY-positive (8, 11), but disrupting *cry* in PDF cells with the *Pdf-Gal4* (7)
154 had only a very small effect on constant light arrhythmicity (Fig. 2D, G, Table S1). In contrast,
155 flies in which *cry* was mutated in the cells marked by the *dvPdf-Gal4* were fully rhythmic,
156 indistinguishable from CRY loss in all circadian neurons (Fig. 2G, Table S1). This is interesting
157 because the *dvPdf-Gal4* labels only 5 more cells per hemibrain than *Pdf-Gal4*, and only 2 of these
158 5 cells are CRY-positive: the 5th sLNv and the one ITP-positive LNd (41, 42).

159 Ongoing work in our lab has characterized two Janelia split-Gal4 drivers, *ss00639-GAL4*
160 and *ss00773-Gal4*. They both specifically label one CRY^{+} LNd and the 5th sLNv in addition to
161 very few additional cells (Fig. S4). Expression of CRISPR reagents against *cry* with the *ss00639-*
162 *Gal4* driver also caused complete rhythmicity in constant light; more than 90% of the flies were
163 rhythmic (Fig. 2E, G, Table S1). Similar but less strong results were seen with *ss00773-Gal4* (Fig
164 2G, Table S1). A third Gal4 driver, *MB122B-Gal4*, also expresses in these same two cells along

165 with two additional LNd cells (43, 44), and mutating *cry* in cells labelled by this driver resulted in
166 about 80% rhythmic flies in constant light (Fig. 2G, Table S1).

167 In addition to the lateral cells, CRY is expressed in the DN1p neurons labeled by the
168 *CLK4.1-Gal4* driver (19, 45). Mutating *cry* in cells labeled by this driver also resulted in potent
169 rhythmicity; nearly 75% of these flies were rhythmic in constant light (Fig. 2F, G, Table S1). These
170 data taken together identify two sets of circadian neurons that can regulate rhythmicity
171 independently under constant light in the absence of CRY: two evening cells consisting of the 5th
172 sLNv and the single ITP-positive LNd as well as the DN1p neurons.

173 To address possible mechanisms underlying the different groups of clock neurons and their
174 regulation of constant light rhythmicity, we examined the circadian period of all rhythmic
175 genotypes. Interestingly, *cry* mutants in all clock neurons have a circadian period of 24.7±0.7h in
176 constant light, about an hour longer than their constant darkness period of 23.6±0.08 h (Fig. 2H,
177 S2E). Mutating CRY in the evening cells with any of the three Gal4s gave rise to a similar period
178 length of greater than 24 h, ~25h (Table S1, green boxes in Fig. 2H). Surprisingly, mutating CRY
179 only in the DN1ps caused a dramatically shorter constant light period of ~22h (Table S1, Fig. 2H).
180 These data indicate that specific clock neurons mediate the constant light effect and that there are
181 interesting differences between the two discrete sets of relevant neurons (See Discussion).

182 In addition to being rhythmic under constant light, *cry* mutants are also deficient in their
183 response to light pulses (46, 47). Control flies experience a delay phase shift in response to a light
184 pulse in the early night at ZT15, an advance phase in response to a light pulse in the late night at
185 ZT21 but little change with a light pulse in the middle of the night at ZT18 (46). The unresponsive
186 *cry* mutant phenotype was reproduced by loss of CRY function specifically in clock neurons (Fig.
187 2I). Interestingly, flies with loss of CRY from PDF neurons were also completely deficient in the

188 ZT15 light pulse-mediated phase delay but still maintained some phase advance induced by the
189 ZT21 light pulse. In addition, when CRY function was perturbed in both PDF neurons and evening
190 cells using the dvPDF-Gal4, the phase advance as well as the phase delay response was abolished
191 (Fig. 2I). However, loss of CRY either in the evening cells alone or in the DN1p neurons did not
192 affect the phase response (Fig. 2J). These data further indicate that CRY functions in discrete sets
193 of clock neurons to mediate diverse light responses (see Discussion).
194
195 **PDF regulates activity and sleep from both the large and small LNvs.**
196 A key circadian molecule beyond the core clock is the neuropeptide pigment dispersing factor
197 (PDF); it is encoded by the gene *Pdf*. Null mutants of the gene (Pdf^{01}) are largely arrhythmic in
198 constant darkness (7). PDF is expressed in only 8 pairs of lateral neurons in the adult brain, four
199 small (sLNvs) and four large (lLNvs) ventral lateral neurons per hemibrain. The lLNvs express
200 very high levels of PDF, which can be easily visualized within their long arborizations. They
201 extend to the optic lobes and to the other side of the brain. The sLNvs extend a long dorsal process,
202 which is also marked by PDF staining (Fig. S5A, (48)).
203 A UAS-3X-gRNA line against *Pdf* (*UAS-Pdf-g*) in combination with the *Pdf-Gal4* driver
204 that labels all PDF-producing neurons caused loss of PDF from the cell bodies and projections of
205 most PDF neurons (Fig. 3A, B and S5B). There was however residual staining in some lLNvs (Fig
206 3A, bottom panel, S5B), which likely reflects some residual PDF due to its very high levels in
207 these cells prior to the mutagenesis. Nonetheless, this strain was completely arrhythmic in constant
208 darkness whereas the parental control strains had normal rhythms (Fig. S6A-C, F). The very few
209 rhythmic flies also had a shorter period phenotype (Fig. S6I).
210 We then used previously described split-Gal4 lines generated by the Rubin lab at Janelia

211 (36) to specifically target only sLNvs or only lLNvs. The CRISPR-Cas9-based method was again
212 highly effective in targeting PDF levels only in the cells targeted by the respective Gal4s.
213 Expression of the gRNA and Cas9 in sLNv-specific driver (*ss00681-Gal4*) led to near complete
214 loss of PDF staining from 100% of the sLNvs examined and their dorsal processes, with no effect
215 on the lLNv cell bodies or on their processes. Similarly, expressing the CRISPR reagents using the
216 lLNv-specific driver (*ss00645-Gal4*) significantly reduced PDF expression from lLNv cell bodies
217 and processes, without affecting PDF levels in the sLNvs or their dorsal process (Fig. 3A, B; S5B).
218 However, the effect on the lLNvs was not as strong: about 20% of the neurons (1-2 neurons from
219 about half the hemibrains) still had unchanged PDF staining. This is very likely because the
220 *ss00645-Gal4* variably labels 3-4 lLNvs per hemisphere. Notably however, there remains some
221 residual staining in the lLNvs even with *Pdf-Gal4* (Fig. 3A, B-bottom panels), probably due to the
222 higher levels of PDF in the lLNvs (see Discussion). As expected based on earlier studies (13), loss
223 of PDF from the sLNvs but not from the lLNvs caused arrhythmicity in constant darkness (Fig.
224 S6D-H).

225 Loss of PDF from both small and large PDF neurons also caused substantially increased
226 sleep under constant darkness (Fig. 3C, F), and targeting the guides specifically to the small cells
227 caused a similar sleep increase (Fig. 3D, G). This increase in sleep is not because of a lack of the
228 ability to move as these flies are even more active than the controls when awake (Table S2).
229 Although a role for PDF neurons in sleep and arousal has been described (6, 49), CRISPR-mediated
230 loss of PDF specifically from the sLNvs here is the most direct evidence that the sLNvs regulate
231 sleep. Loss of PDF from only the large cells also increased sleep but to a much smaller extent (Fig.
232 3E, H). Although the difference between the small and large cells may be due to the residual large
233 cell PDF that escapes knockdown, or perhaps to the few lLNvs not labelled by the split-Gal4 driver,

234 the very significant reduction in PDF signal from lLNv cell bodies and processes in most brains
235 (Fig 3A-B, bottom panels; S5B) makes it more likely that the lLNvs have a smaller role in
236 regulating sleep than the sLNvs in constant darkness.

237 An analysis of sleep structure indicated a substantial decrease in p-wake (the instantaneous
238 probability that the flies will awaken from sleep), but no effect on p-doze (the instantaneous
239 probability that awake flies will fall asleep (50)) (Fig. 3I-K, Table S2). These data are consistent
240 with a wake-promoting role of PDF (6) and identify PDF from the sLNvs as the primary regulator.
241

242 **Temporally regulated CRISPR-Cas9 mutagenesis assigns PDF function to adult neurons.**
243 The function of several circadian genes has not yet been definitively assigned to the adult fly, so
244 some of them might have a substantial developmental role. Traditional methods of temporal
245 regulation of Gal4 activity such as GeneSwitch (51) or the temperature-sensitive Gal80 system
246 (52) are not ideal for behavior experiments as they either involve toxic drugs or dramatic shifts in
247 temperature, both of which severely impact the standard locomotor behavior assay (53, 54).
248 Pairing with the temperature sensitive Gal80 system also resulted in leaky mutagenesis (33). We
249 therefore assessed two more recently developed methods, one specific to CRISPR and the other
250 more general, to mutagenize genes of interest adult-specifically.

251 The first was the inducible Cas9 method developed by Port et. al. (33). It is a UAS-based
252 method: the Cas9 sequence is preceded by a GFP cassette, which is followed by a STOP codon
253 flanked by FRT sites (hereafter called STOP-Cas9). Pairing with a heat-shock induced flp
254 transgene allows for temporal control of mutagenesis as Cas9 expression occurs only post heat
255 shock (Fig. S7A). We adapted this method for adult-specific induction by using three consecutive
256 heat shocks (referred to below as "heat shock"; see Methods). Since these heat shocks are

257 temporally separated by several days from the behavior analyses, the heat shocks are not expected
258 to alter circadian behavior. The STOP-Cas9 transgene was combined with *Pdf-Gal4*, *UAS-Pdf-g,*
259 a *UAS-mRFP* transgene to label the PDF cells as well as a heat shock induced flp encoding
260 hsFLPG5 (Fig. S7A).

261 In control flies without *UAS-Pdf-g*, heat shock did not affect the levels of PDF (Fig. 4A, B,
262 S7B) and did not negatively impact rhythmic behavior (Fig. 4C, D). Importantly, flies expressing
263 all the transgenes including the UAS-gRNA but without heat shock showed no loss of PDF signal
264 (Fig. 4A, B, S7B) and no defects in behavior (Fig. 4C-F); this indicates no leaky expression without
265 heat shock. In the same flies two weeks post heat shock, PDF staining was lost from all sLNvs in
266 ~60% of the hemibrains analyzed, whereas some mosaicism was observed in the remaining 40%
267 of the hemibrains; 1-2 neurons still expressed both GFP and PDF (Fig. 4A, B; S7B). A similar
268 fraction of the heat shocked mutant flies, about 38 percent, were rhythmic in constant darkness
269 (Fig. 4D, S7C), indicating an adult-specific requirement of PDF for rhythmicity. The ca. 60 percent
270 arrhythmic flies also showed an adult-specific effect of PDF on sleep (Fig. 4E).

271 The remaining rhythmic flies likely reflect mosaicism, as PDF from 1-2 neurons might be
272 sufficient to maintain some level of rhythmicity. This is supported by the fact that the rhythmicity
273 and sleep phenotypes were correlated in the mutant flies (Fig. S7D). Surprisingly, heat shock alone
274 had a strong effect on the sleep structure and lowered p-wake significantly in the controls.
275 Therefore, no conclusions could be drawn about the adult-specific effect of PDF in maintaining p-
276 wake (Fig. 4F). These data indicate that the heat-shock based methods are compatible with
277 studying circadian behavior but may be less suitable for studying sleep behavior.

278 We also combined CRISPR-Cas9 mutagenesis with a more general method of temporal
279 regulation that affects the Gal4 and therefore controls all UAS-based strategies, the recently

280 developed auxin-inducible gene expression system (AGES, (55)). It uses the traditional Gal4
281 repressor Gal80, which has been engineered to be regulated by auxin. Auxin is non-toxic and does
282 not affect fly lifespan at the required concentrations (55). We combined the AGES system with the
283 regular Cas9, *UAS-Cas9.P2,* along with *UAS-Pdf-g* and *UAS-mRFP* to label the LNvs with the
284 *Pdf-Gal4* driver (Fig. S8A).

285 AGES sequesters GAL4 and thus inhibits expression from all UAS-transgenes without
286 auxin feeding (Fig. S8A, (55)). Indeed, there is no to very low mRFP expression in cell bodies or
287 processes without auxin feeding (Fig. 5A, S8B). However, expression must be non-zero, as some
288 PDF mutagenesis is observed without auxin feeding (~2-fold reduction in PDF levels, Fig. 5A, B).
289 Not surprisingly, auxin feeding leads to a much bigger effect - near loss of all PDF from cell bodies
290 (>10-fold reduction) as well as processes (Fig. 5A, B, S8B).

291 The small-scale leaky mutagenesis without auxin feeding had only a minor effect on
292 rhythmicity and sleep (Fig. 5C, D, E). However, auxin feeding caused a very strong effect on both
293 rhythmicity and sleep just like the effect on PDF staining (Fig. 5D, E, S8C), and adult-specific loss
294 of PDF lowered p-wake (Fig. 5F). Auxin feeding alone in control flies had a very minor effect on
295 PDF staining (20% reduction in cell bodies) and no effect on circadian behavior and sleep duration
296 (Fig. 5A-E, S8B, C). There was also a significant interaction between auxin feeding and expression
297 of CRISPR reagents against PDF on p-wake ($p<0.001$, Two-way ANOVA; Fig 5F). Combining
298 AGES with the CRISPR system therefore indicate that most if not all aspects of PDF function on
299 circadian behavior and sleep are adult-specific.

300 We then assayed the time required for adult-specific-CRISPR mediated mutagenesis. Flies
301 expressing *UAS-Cas9.P2* and *UAS-Pdf-g* along with AGES were fed 10mM auxin for 2-, 4- and
302 7-days before testing for behavior on food without auxin. 2 days of auxin feeding did not

303 significantly alter rhythmicity of the controls, but there was a gradual reduction in rhythmicity
304 from 4 days to 7 days of auxin feeding (Fig. 5G). To further tease apart the required time for
305 CRISPR mutagenesis from the effects of protein turnover, we used the same paradigm to test two
306 proteins that undergo daily degradation – CRY and PER. For both proteins, 2 days of auxin feeding
307 was sufficient to cause a phenotype indistinguishable from the perturbations through development
308 (Fig. 5H, I), indicating that no more than 2 days are required for mutagenesis.
309
310
311
312
313
314

315 **Discussion**

316 In this study we generated new UAS-3X-gRNA lines for neuron-specific perturbation of three key
317 circadian genes and combined them with defined Gal4 drivers to assay their function in specific
318 subsets of clock neurons. We could reproduce the mutant phenotypes of *vri, cry* and *Pdf* in known
319 neurons and identified previously unknown cell type-specific functions of these genes. The
320 approach worked very well with specific and weak Gal4 drivers, which allowed the discovery of
321 two subsets of circadian neurons within which CRY acts independently to regulate rhythmicity
322 under constant light conditions. Finally, these new reagents were compatible with existing tools
323 and shown to be highly effective with two independent methods for temporal regulation. The
324 results and lines described here will be of use to the circadian community, but we hope that the
325 detailed validation of the method will appeal to a much wider population of fly neuroscientists and
326 encourage them to switch from the standard but less dependable RNAi methodology to this more
327 effective and consistent method for the spatial and temporal knockout of genes in adult fly neurons.

328 Our data show that this cell type-specific CRISPR method works well with highly
329 expressed genes like *Pdf* and even with weak split-Gal4 drivers. It is also ideal for addressing the
330 adult function of essential genes such as *vri*, by perturbing their expression levels and function in
331 inessential cells as we show here for circadian neurons. In this context, the functions of many
332 *Drosophila* genes are defined only in developmental contexts, even though these same genes are
333 expressed again in adults. For example, we recently found that genes encoding GPCRs,
334 transcription factors and cell surface molecules are broadly yet specifically expressed in clock and
335 dopaminergic neurons. Studying their function in these specific adult neurons is beginning to help
336 define the molecular underpinnings of neural circuits and behavior (23, 56). Towards these goals,
337 we have generated and begun to use a library of guideRNA lines against all GPCRs expressed in

338 *Drosophila* (37). Moreover, several lines with 2X-gRNA generated by Port and Boutros (33) are
339 now publicly available. Such resources should also make this method a first choice for tissue and
340 cell type-specific reverse genetic screens.

341 Another novel application of this method should be cell-specific gene-interaction studies.
342 Combining multiple RNAi lines is not common, perhaps because of the suspected dilution effects
343 of multiple UAS lines. In contrast, this CRISPR-Cas9 method does not require high expression
344 levels, so combining gRNAs against multiple genes, for example to study enhancer and suppressor
345 phenotypes, should be possible and would extend the approach in an interesting direction.

346 VRI operates as a part of the molecular transcription translation feedback loop that operates
347 in clock neurons (57). Hemizygous mutants of *vri* are rhythmic with a short circadian period (4).
348 Concurrently, a recent study generated a new homozygous mutant that has normal rhythms with a
349 short circadian period despite dramatically reduced VRI levels in the clock neurons (40). These
350 results are in complete agreement with ours (Fig. 1C-G). It is also possible that very low levels of
351 VRI in clock neurons is sufficient to maintain rhythms like in the whole body mutant (40).
352 Although unlikely in our view, this interpretation is consistent with an earlier study (58). It used
353 cell-specific flip outs of a rescue transgene in a mutant *vri* background and found that VRI in PDF
354 neurons regulates rhythmicity, but this result could have been influenced by the mutant background
355 (58). Although over-expression of VRI also results in considerable loss of rhythms (4), simple loss
356 of function via these CRISPR-Cas9-based methods is less prone to misinterpretation than gain-of-
357 function experiments. In the future, guides can be targeted to specific subsets of circadian and non-
358 circadian cells to further define the function of VRI in the regulation of development and behavior.

359 The CRY photoreceptor along with the compound eyes and H-B eyelets are the three
360 pathways through which flies entrain to environmental light cues (59). It is therefore not surprising

361 that *cry* mutants are still able to light entrain normally. However, these mutants are rhythmic under
362 constant bright light conditions, indicating a special role for CRY under prolonged light exposure
363 conditions (12). CRY is expressed in several different clock neurons; they include the PDF
364 neurons, a subset of evening cells (5th sLNv+3 LNds) and a subset of the DN1ps (8). Interestingly,
365 we find that CRY only functions in the evening cells and the DN1ps to regulate the response to
366 constant light. This conclusion agrees with previous results indicating that evening cells (60, 61)
367 and dorsal neurons (60, 62) are the principal drivers of rhythmicity under constant light conditions.
368 QSM is another protein that mediates light input to the circadian clock, and flies mutant for QSM
369 in dorsal neurons maintain rhythmicity in constant light (63), further emphasizing the role of dorsal
370 neurons in mediating rhythmicity under constant light conditions.

371 Our results also agree with earlier results that PDF positive LNvs have no more than a
372 minor role in responding to constant light (61, 62). Because the sLNvs are directly downstream of
373 the light responsive H-B eyelets (64), these neurons may be constantly electrically stimulated and
374 their molecular clock therefore poisoned by constant light even without CRY. In contrast, loss of
375 CRY in either of the two other major subsets of CRY-positive neurons, the two evening cells (5th
376 sLNv, CRY^+ and ITP^+ LNd) as well as the DN1ps, is sufficient to maintain rhythmicity in constant
377 light. These data indicate that CRY may be the primary source of light information in these
378 neurons; perhaps they are critical for adapting to altered photoperiods such as longer summer days.

379 Interestingly, CRY functions in a different subset of clock neurons, the PDF neurons, to
380 effect light pulse-mediated phase delays in the early night. Phase delays induced by a light pulse
381 in the late night also requires CRY in PDF neurons but additionally requires CRY in evening
382 neurons (Fig. 2I). A CRY requirement for phase responses in PDF neurons has been previously
383 described (65), and a role for the evening neurons in phase response behavior has also been

384 suggested (60). As neuronal activation of PDF neurons at different times of day can mimic a light-
385 mediated phase response curve in a CRY independent manner (66), CRY photon capture may
386 impact neuronal firing, a result consistent with direct observation (67), so altered electrical
387 properties of the CRY mutants might also contribute to the observed light-mediated phenotypes.

388 Expression of *UAS-Cas9* and *UAS-Pdf-g* with *Pdf-Gal4* resulted in complete loss of PDF
389 from sLNvs but only partial loss from the lLNvs (Fig. 3A, B). The higher levels of PDF in lLNvs
390 than in sLNvs is one possible explanation, but persistent PDF in lLNvs might also reflect the
391 duration of expression of the CRISPR tools in the different cells. The sLNvs have an early larval
392 origin, well before the lLNvs appear in the mid-late pupal stage (48). This temporal pattern is
393 recapitulated by *Pdf-Gal4* (7), allowing sLNvs a much longer time for mutagenesis and subsequent
394 protein turnover.

395 PDF is a key circadian neuropeptide in *Drosophila*, and the small PDF neurons (sLNvs)
396 are critical for circadian behavior (14, 15). This is because PDF from the sLNvs is a key regulator
397 of rhythmicity in constant darkness (13). The results here show that loss of PDF from these neurons
398 also has a major effect on sleep structure, namely, a decrease in p-wake. Loss of PDF from the
399 lLNvs has a qualitatively similar but much smaller quantitative decrease in p-wake (Fig. 3I- K).
400 This indicates that PDF from both sources is wake-promoting, consistent with the fact that
401 activation of lLNvs mediates arousal (18, 49). A greater role for lLNvs has been described in
402 promoting wake through GABA signaling under light-dark conditions (68, 69). It is therefore
403 possible that the lLNvs play a larger role in maintaining wakefulness under LD conditions, whereas
404 rhythmic PDF release from the sLNvs in constant darkness promotes wake as well as maintains
405 rhythmicity.

406 Two independent methods indicate that PDF functions adult-specifically to regulate
407 rhythmicity and sleep. Although both worked effectively, the two strategies have distinguishing
408 features. The inducible Cas9 system was very robust i.e., there was no leaky expression, which
409 provides high confidence in the adult-specific conclusion. However, the induction was incomplete,
410 leading to some mosaicism and considerable variability in the resulting phenotypes (Fig. S7A).
411 Perhaps this could be solved by further altering the heat shock regimen, especially for rhythmicity
412 as this assay is insensitive to the brief heat shock. Effects on sleep were more problematic, as even
413 sleep in the control flies was impacted by heat shock (Fig. 4F). It is presently uncertain if the effect
414 of heat shock alone on sleep structure is strain-specific or a more general effect.

415 In contrast to heat shock, the AGES system was highly efficient but exhibited some
416 background mutagenesis in the absence of auxin at least with the PDF-Gal4 driver. As the AGES
417 system was highly effective at inhibiting expression of a fluorescent protein marker (Fig. 5A, S8B),
418 the background mutagenesis likely reflects the ability of even very low levels of Cas9 and gRNA
419 expression to induce mutagenesis as well as the sensitivity of this assay. The lack of a similar leaky
420 phenotype with the CLK856-Gal4 driver (Fig. 5G) suggests that it is Gal4-specific. Perhaps the
421 CLK856-Gal4 driver only labels the PDF neurons at a later developmental stage, allowing less
422 time to effect the leaky phenotype. Although mutagenesis sensitivity is a potential liability in this
423 specific context, it is a generally positive feature of the CRISPR-based system: it does not require
424 that drivers be highly expressed to mediate efficient mutagenesis. In the context of AGES, the use
425 of lower expression Cas9 variants (33) might circumvent this issue. Importantly, auxin exposure
426 alone had no detectable effect on circadian or sleep behavior (Fig. 5E, F). Thus, we find auxin
427 exposure to be a less disruptive perturbation than heat shock and hence a mode of CRISPR
428 induction more compatible for behavior analyses. Moreover, temporal regulation via AGES allows

429 combining with other UAS transgenes for experiments like complementation analysis. Although
430 the current version of AGES is incompatible with the many Gal80-insensitive split-Gal4 lines (25),
431 it can be used with new Gal80-sensitive split-Gal4 lines (70). In summary, both temporal methods
432 are effective, and we hope this exploration of their differences will help researchers choose the one
433 best suited to their needs.
434

435 **Materials and Methods**
436
437 **Fly Stocks and Rearing**

438 All flies were raised on a standard cornmeal media supplemented with yeast in a temperature
439 controlled incubator at 25°C in 12:12 Light:Dark cycles. The genotypes of all fly strains used in
440 this study are listed in supplementary Table S3. Details on fly lines generated in this study are
441 described in SI Appendix, Materials and Methods, Generation of Fly Lines.

442

443 **Locomotor Activity and Sleep Behavior**

444 For behavior analysis of flies with throughout (not adult-specific) perturbations, 0-3 days old male
445 flies of the appropriate genotype were collected and aged till they were about 2 weeks old at 25°C
446 in 12:12 LD, with food changes every 3-4 days. The flies were then loaded into behavior tubes
447 containing food (4% sucrose and 2% agar) and loaded onto *Drosophila* Activity Monitors (DAM;
448 TriKinetics Inc., Waltham, MA). These DAMs were placed in light boxes with programmable LED
449 light intensities inside a temperature-controlled incubator set to 25°C. Flies were entrained for 2-3
450 days with 12h:12h lights ON (500 lux): lights OFF before being switched to either constant
451 darkness or constant light (500 lux). Circadian rhythmicity and sleep analysis was performed using
452 the 2020 version of Sleep and Circadian Analysis MATLAB Program (SCAMP) developed by
453 Christopher G. Vecsey (71).Details of locomotor behavior analysis are described in SI Appendix,
454 Materials and Methods, Locomotor Activity and Sleep Behavior.

455

456 **Immunohistochemistry**

457 Whole flies of the same genotype and age as the behavior experiment cohort were fixed in 4%
458 paraformaldehyde. Dissected brains were washed and blocked with 10% Normal Goat Serum

459 (NGS; Jackson labs). The following primary antibodies were used diluted in blocking buffer–
460 chicken anti-GFP (Abcam ab13970; 1:1000), mouse anti-PDF (DSHB-PDF C7; 1:1000), guinea
461 pig anti-VRI (gift of Paul Hardin; 1:3000 (72)), rat anti-TIM (Rosbash lab; 1:250), rabbit anti-
462 dsRed (Takara Bio- 632393; 1:300), rabbit anti-PER (Rosbash lab, 1:1000), rat anti-CRY (Rosbash
463 lab, 1:200) and rat anti-RFP (Proteintech-5f8; 1:1000). Further details on image acquisition and
464 analysis can be found in SI Appendix, Materials and Methods, Immunohistochemistry and Image
465 Analysis.
466
467 See also, SI Appendix, Materials and Methods, Data representation and Statistics.
468
469
470
471
472
473
474
475
476

Acknowledgements

We thank Michelle Lin for assistance with maintaining fly stocks. We thank Matthias Schlichting and all members of the Rosbash lab for useful discussions. We thank Paul Garrity, Justin Blau and Katharine Abruzzi for helpful comments on the manuscript. We thank Paul Hardin for the VRI antibody. We thank Heather Dionne, Aljoscha Nern and Gerry Rubin (Janelia Research campus) for the split-Gal4 lines, and Filip Port and Michael Boutros for the STOP-Cas9 flies. Stocks obtained from the Bloomington Drosophila Stock Center (NIH P40OD018537) and Vienna Drosophila Resource Center (VDRC) were used in this study. This work was supported by the Howard Hughes Medical Institute (HHMI).

487 **References**

488 1. R. Allada, B. Y. Chung, Circadian Organization of Behavior and Physiology in
489 Drosophila. *Annu. Rev. Physiol.* **72**, 605–624 (2010).

490 2. P. E. Hardin, Molecular genetic analysis of circadian timekeeping in Drosophila.
491 *Adv. Genet.* **74**, 141–173 (2011).

492 3. C. Helfrich-Förster, The neuroarchitecture of the circadian clock in the brain of
493 Drosophila melanogaster. *Microsc. Res. Tech.* **62**, 94–102 (2003).

494 4. J. Blau, M. W. Young, Cycling vrille expression is required for a functional
495 Drosophila clock. *Cell* **99**, 661–671 (1999).

496 5. J. Benito, H. Zheng, P. E. Hardin, PDP1ε Functions Downstream of the Circadian
497 Oscillator to Mediate Behavioral Rhythms. *J. Neurosci.* **27**, 2539–2547 (2007).

498 6. K. M. Parisky, *et al.*, PDF cells are a GABA-responsive wake-promoting component
499 of the Drosophila sleep circuit. *Neuron* **60**, 672–682 (2008).

500 7. S. C. Renn, J. H. Park, M. Rosbash, J. C. Hall, P. H. Taghert, A pdf neuropeptide
501 gene mutation and ablation of PDF neurons each cause severe abnormalities of
502 behavioral circadian rhythms in Drosophila. *Cell* **99**, 791–802 (1999).

503 8. J. Benito, J. H. Houl, G. W. Roman, P. E. Hardin, The blue light photoreceptor
504 CRYPTOCHROME is expressed in a subset of circadian oscillator neurons in the
505 Drosophila CNS. *J. Biol. Rhythms* **23**, 296–307 (2008).

506 9. P. Emery, W. V. So, M. Kaneko, J. C. Hall, M. Rosbash, CRY, a Drosophila Clock
507 and Light-Regulated Cryptochrome, Is a Major Contributor to Circadian Rhythm
508 Resetting and Photosensitivity. *Cell* **95**, 669–679 (1998).

509 10. R. Stanewsky, *et al.*, The cryb mutation identifies cryptochrome as a circadian
510 photoreceptor in Drosophila. *Cell* **95**, 681–692 (1998).

511 11. T. Yoshii, T. Todo, C. Wülbeck, R. Stanewsky, C. Helfrich-Förster, Cryptochrome
512 is present in the compound eyes and a subset of Drosophila's clock neurons. *J.*
513 *Comp. Neurol.* **508**, 952–966 (2008).

514 12. P. Emery, R. Stanewsky, J. C. Hall, M. Rosbash, A unique circadian-rhythm
515 photoreceptor. *Nature* **404**, 456–457 (2000).

516 13. O. T. Shafer, P. H. Taghert, RNA-Interference Knockdown of Drosophila Pigment
517 Dispersing Factor in Neuronal Subsets: The Anatomical Basis of a Neuropeptide's
518 Circadian Functions. *PLOS ONE* **4**, e8298 (2009).

519 14. B. Grima, E. Chélot, R. Xia, F. Rouyer, Morning and evening peaks of activity rely
520 on different clock neurons of the Drosophila brain. *Nature* **431**, 869–873 (2004).

521 15. D. Stoleru, Y. Peng, J. Agosto, M. Rosbash, Coupled oscillators control morning
522 and evening locomotor behaviour of Drosophila. *Nature* **431**, 862–868 (2004).

523 16. Z. Yao, O. T. Shafer, The Drosophila circadian clock is a variably coupled network
524 of multiple peptidergic units. *Science* **343**, 1516–1520 (2014).

525 17. C. Dubowy, A. Sehgal, Circadian Rhythms and Sleep in Drosophila melanogaster.
526 *Genetics* **205**, 1373–1397 (2017).

527 18. Y. Shang, L. C. Griffith, M. Rosbash, Light-arousal and circadian photoreception
528 circuits intersect at the large PDF cells of the Drosophila brain. *Proc. Natl. Acad.*
529 *Sci.* **105**, 19587–19594 (2008).

530 19. L. Zhang, *et al.*, DN1p Circadian Neurons Coordinate Acute Light and PDF Inputs
531 to Produce Robust Daily Behavior in Drosophila. *Curr. Biol.* **20**, 591–599 (2010).

532 20. F. Guo, *et al.*, Circadian neuron feedback controls the Drosophila sleep–activity
533 profile. *Nature* **536**, 292–297 (2016).

534 21. F. Guo, M. Holla, M. M. Díaz, M. Rosbash, A Circadian Output Circuit Controls
535 Sleep-Wake Arousal in Drosophila. *Neuron* **100**, 624-635.e4 (2018).

536 22. A. N. King, A. Sehgal, Molecular and circuit mechanisms mediating circadian clock
537 output in the Drosophila brain. *Eur. J. Neurosci.* **51**, 268–281 (2020).

538 23. D. Ma, *et al.*, A transcriptomic taxonomy of Drosophila circadian neurons around
539 the clock. *eLife* **10**, e63056 (2021).

540 24. A. H. Brand, N. Perrimon, Targeted gene expression as a means of altering cell fates
541 and generating dominant phenotypes. *Dev. Camb. Engl.* **118**, 401–415 (1993).

542 25. H. Luan, N. C. Peabody, C. R. Vinson, B. H. White, Refined Spatial Manipulation
543 of Neuronal Function by Combinatorial Restriction of Transgene Expression.
544 *Neuron* **52**, 425–436 (2006).

545 26. G. W. Meissner, *et al.*, A searchable image resource of Drosophila GAL4-driver
546 expression patterns with single neuron resolution. 2020.05.29.080473 (2022).

547 27. M. Sekiguchi, K. Inoue, T. Yang, D.-G. Luo, T. Yoshii, A Catalog of GAL4 Drivers
548 for Labeling and Manipulating Circadian Clock Neurons in Drosophila
549 melanogaster. *J. Biol. Rhythms* **35**, 207–213 (2020).

550 28. G. Dietzl, *et al.*, A genome-wide transgenic RNAi library for conditional gene
551 inactivation in Drosophila. *Nature* **448**, 151–156 (2007).

552 29. H. Meltzer, *et al.*, Tissue-specific (ts)CRISPR as an efficient strategy for in vivo
553 screening in Drosophila. *Nat. Commun.* **10**, 2113 (2019).

554 30. F. Port, H.-M. Chen, T. Lee, S. L. Bullock, Optimized CRISPR/Cas tools for
555 efficient germline and somatic genome engineering in Drosophila. *Proc. Natl. Acad.*
556 *Sci. U. S. A.* **111**, E2967-2976 (2014).

557 31. F. Port, M. Boutros, Tissue-Specific CRISPR-Cas9 Screening in Drosophila.
558 *Methods Mol. Biol. Clifton NJ* **2540**, 157–176 (2022).

559 32. M. Jinek, *et al.*, A Programmable Dual-RNA–Guided DNA Endonuclease in
560 Adaptive Bacterial Immunity. *Science* **337**, 816–821 (2012).

561 33. F. Port, *et al.*, A large-scale resource for tissue-specific CRISPR mutagenesis in
562 Drosophila. *eLife* **9**, e53865 (2020).

563 34. F. Port, S. L. Bullock, Augmenting CRISPR applications in Drosophila with tRNA-
564 flanked sgRNAs. *Nat. Methods* **13**, 852–854 (2016).

565 35. R. Delventhal, *et al.*, Dissection of central clock function in Drosophila through cell-
566 specific CRISPR-mediated clock gene disruption. *eLife* **8**, e48308 (2019).

567 36. M. Schlichting, M. M. Díaz, J. Xin, M. Rosbash, Neuron-specific knockouts indicate
568 the importance of network communication to Drosophila rhythmicity. *eLife* **8**,
569 e48301 (2019).

570 37. M. Schlichting, *et al.*, Dopamine and GPCR-mediated modulation of DN1 clock
571 neurons gates the circadian timing of sleep. *Proc. Natl. Acad. Sci.* **119**, e2206066119
572 (2022).

573 38. H. George, R. Terracol, The vrille Gene of Drosophila Is a Maternal Enhancer of
574 decapentaplegic and Encodes a New Member of the bZIP Family of Transcription
575 Factors. *Genetics* **146**, 1345–1363 (1997).

576 39. A. Matsumoto, *et al.*, A functional genomics strategy reveals *clockwork orange* as
577 a transcriptional regulator in the *Drosophila* circadian clock. *Genes Dev.* **21**, 1687–
578 1700 (2007).

579 40. K. L. Gunawardhana, G. B. S. Rivas, C. Caster, P. E. Hardin, Crosstalk between
580 vrille transcripts, proteins, and regulatory elements controlling circadian rhythms
581 and development in Drosophila. *iScience* **24** (2021).

582 41. J. H. Bahn, G. Lee, J. H. Park, Comparative Analysis of Pdf-Mediated Circadian
583 Behaviors Between Drosophila melanogaster and D. virilis. *Genetics* **181**, 965–975
584 (2009).

585 42. F. K. Schubert, N. Hagedorn, T. Yoshii, C. Helfrich-Förster, D. Rieger,
586 Neuroanatomical details of the lateral neurons of Drosophila melanogaster support
587 their functional role in the circadian system. *J. Comp. Neurol.* **526**, 1209–1231
588 (2018).

589 43. N. Bulthuis, K. R. Spontak, B. Kleeman, D. J. Cavanaugh, Neuronal Activity in
590 Non-LNv Clock Cells is Required to Produce Free-Running Rest:Activity Rhythms
591 in Drosophila. *J. Biol. Rhythms* **34**, 249–271 (2019).

592 44. F. Guo, X. Chen, M. Rosbash, Temporal calcium profiling of specific circadian
593 neurons in freely moving flies. *Proc. Natl. Acad. Sci. U. S. A.* **114**, E8780–E8787
594 (2017).

595 45. Y. Zhang, Y. Liu, D. Bilodeau-Wentworth, P. E. Hardin, P. Emery, Light and
596 Temperature Control the Contribution of Specific DN1 Neurons to Drosophila
597 Circadian Behavior. *Curr. Biol. CB* **20**, 600–605 (2010).

598 46. C. Kistenpfennig, J. Hirsh, T. Yoshii, C. Helfrich-Förster, Phase-shifting the fruit
599 fly clock without cryptochrome. *J. Biol. Rhythms* **27**, 117–125 (2012).

600 47. P. Vinayak, *et al.*, Exquisite Light Sensitivity of Drosophila melanogaster
601 Cryptochrome. *PLOS Genet.* **9**, e1003615 (2013).

602 48. C. Helfrich-Förster, Development of pigment-dispersing hormone-immunoreactive
603 neurons in the nervous system of Drosophila melanogaster. *J. Comp. Neurol.* **380**,
604 335–354 (1997).

605 49. V. Sheeba, *et al.*, Large Ventral Lateral Neurons Modulate Arousal and Sleep in
606 Drosophila. *Curr. Biol. CB* **18**, 1537–1545 (2008).

607 50. T. D. Wiggin, *et al.*, Covert sleep-related biological processes are revealed by
608 probabilistic analysis in Drosophila. *Proc. Natl. Acad. Sci. U. S. A.* **117**, 10024–
609 10034 (2020).

610 51. T. Osterwalder, K. S. Yoon, B. H. White, H. Keshishian, A conditional tissue-
611 specific transgene expression system using inducible GAL4. *Proc. Natl. Acad. Sci.*
612 **98**, 12596–12601 (2001).

613 52. S. E. McGuire, Z. Mao, R. L. Davis, Spatiotemporal gene expression targeting with
614 the TARGET and gene-switch systems in Drosophila. *Sci. STKE Signal Transduct.*
615 *Knowl. Environ.* **2004**, pl6 (2004).

616 53. Q. Li, N. Stavropoulos, Evaluation of Ligand-Inducible Expression Systems for
617 Conditional Neuronal Manipulations of Sleep in Drosophila. *G3*
618 *GenesGenomesGenetics* **6**, 3351–3359 (2016).

619 54. K. M. Parisky, J. L. Agosto Rivera, N. C. Donelson, S. Kotecha, L. C. Griffith,
620 Reorganization of Sleep by Temperature in Drosophila Requires Light, the
621 Homeostat, and the Circadian Clock. *Curr. Biol. CB* **26**, 882–892 (2016).

622 55. C. D. McClure, *et al.*, An auxin-inducible, GAL4-compatible, gene expression
623 system for Drosophila. *eLife* **11**, e67598 (2022).

624 56. D. Ma, *et al.*, Neural connectivity molecules best identify the heterogeneous clock
625 and dopaminergic cell types in the Drosophila adult brain. *Sci. Adv.* **9**, eade8500
626 (2023).

627 57. S. A. Cyran, *et al.*, vrille, Pdp1, and dClock Form a Second Feedback Loop in the
628 Drosophila Circadian Clock. *Cell* **112**, 329–341 (2003).

629 58. K. L. Gunawardhana, P. E. Hardin, VRILLE Controls PDF Neuropeptide
630 Accumulation and Arborization Rhythms in Small Ventrolateral Neurons to Drive
631 Rhythmic Behavior in Drosophila. *Curr. Biol.* **27**, 3442-3453.e4 (2017).

632 59. C. Helfrich-Förster, C. Winter, A. Hofbauer, J. C. Hall, R. Stanewsky, The
633 Circadian Clock of Fruit Flies Is Blind after Elimination of All Known
634 Photoreceptors. *Neuron* **30**, 249–261 (2001).

635 60. D. Stoleru, *et al.*, The Drosophila Circadian Network Is a Seasonal Timer. *Cell* **129**,
636 207–219 (2007).

637 61. M. Picot, P. Cusumano, A. Klarsfeld, R. Ueda, F. Rouyer, Light activates output
638 from evening neurons and inhibits output from morning neurons in the Drosophila
639 circadian clock. *PLoS Biol.* **5**, e315 (2007).

640 62. A. Murad, M. Emery-Le, P. Emery, A Subset of Dorsal Neurons Modulates
641 Circadian Behavior and Light Responses in Drosophila. *Neuron* **53**, 689–701
642 (2007).

643 63. K. F. Chen, N. Peschel, R. Zavodska, H. Sehadova, R. Stanewsky, QUASIMODO,
644 a Novel GPI-anchored zona pellucida protein involved in light input to the
645 Drosophila circadian clock. *Curr. Biol. CB* **21**, 719–729 (2011).

646 64. M. Schlichting, *et al.*, A Neural Network Underlying Circadian Entrainment and
647 Photoperiodic Adjustment of Sleep and Activity in Drosophila. *J. Neurosci.* **36**,
648 9084–9096 (2016).

649 65. C.-H. A. Tang, E. Hinteregger, Y. Shang, M. Rosbash, Light-Mediated TIM
650 Degradation within Drosophila Pacemaker Neurons (s-LNvs) Is Neither Necessary
651 nor Sufficient for Delay Zone Phase Shifts. *Neuron* **66**, 378–385 (2010).

652 66. F. Guo, I. Cerullo, X. Chen, M. Rosbash, PDF neuron firing phase-shifts key
653 circadian activity neurons in Drosophila. *eLife* **3**, e02780 (2014).

654 67. K. J. Fogle, K. G. Parson, N. A. Dahm, T. C. Holmes, CRYPTOCHROME Is a
655 Blue-Light Sensor That Regulates Neuronal Firing Rate. *Science* **331**, 1409–1413
656 (2011).

657 68. S. Liu, *et al.*, WIDE AWAKE Mediates the Circadian Timing of Sleep Onset.
658 *Neuron* **82**, 151–166 (2014).

69. Y. Li, *et al.*, Drosophila neuroligin 4 regulates sleep through modulating GABA transmission. *J. Neurosci. Off. J. Soc. Neurosci.* **33**, 15545–15554 (2013).

70. B. Ewen-Campen, *et al.*, split-intein Gal4 provides intersectional genetic labeling that is fully repressible by Gal80. 2023.03.24.534001 (2023).

71. N. Donelson, *et al.*, High-Resolution Positional Tracking for Long-Term Analysis of Drosophila Sleep and Locomotion Using the "Tracker" Program. *PLOS ONE* **7**, e37250 (2012).

72. N. R. J. Glossop, *et al.*, VRILLE feeds back to control circadian transcription of Clock in the Drosophila circadian oscillator. *Neuron* **37**, 249–261 (2003).

670 **Figure Legends**

671

672 **Fig. 1: Loss of VRI from clock neurons leads to a shorter circadian period.**

673 **A**. Representative images of large LNV neurons stained for GFP and VRI at ZT19. There is loss
674 of (nuclear) VRI staining in cells expressing both *UAS-Cas9* and UAS-3X-guides against *vri*
675 *(UAS-vri-g)*. Some non-nuclear staining is visible in both control and mutant cells which could be
676 due to background reactivity of the antibody. Scale bar represents 10µm. **B.** Quantification of VRI
677 staining intensity from large LNv neurons represented as a boxplot, n ≥ 36 cells from at least 12
678 hemibrains per genotype, letters represent statistically distinct groups; p<0.001, Kruskal Wallis
679 test followed by a post hoc Dunn's test**. C-E**. Actograms represent double-plotted average activity
680 of flies from an experiment across multiple days. Yellow panel indicates lights ON. **F.** Rhythmicity
681 Index for individual flies plotted as a boxplot, n ≥ 62 per genotype from at least two independent
682 experiments. No statistical difference was observed among the groups tested (p=0.6, Kruskal
683 Wallis test). **G.** Free running period under constant darkness for individual rhythmic flies
684 (RI>0.25) plotted as a boxplot, letters represent statistically distinct groups; p<0.01, Kruskal
685 Wallis test followed by a post hoc Dunn's test.

686

687

688 **Fig. 2: CRY function in two discrete subsets of clock neurons can regulate rhythmicity under**
689 **constant light conditions. A-F**. Actograms represent double-plotted average activity of flies from
690 an experiment across multiple days in constant light. Flies expressing both *UAS-Cas9* and UAS-
691 3X-guides against *cry (UAS-cry-g)* in clock neurons are rhythmic in constant light conditions. **G**.
692 Rhythmicity Index of individual flies quantified for LL2-7 represented by a boxplot, n ≥ 51 per
693 genotype from at least two independent experiments. Letters represent statistically distinct groups;
694 p<0.001, Kruskal Wallis test followed by a post hoc Dunn's test. **H**. Period under constant light
695 for individual rhythmic flies (Rhythmicity Index > 0.25) quantified for LL2-7 represented by a
696 boxplot, letters represent statistically distinct groups; p<0.01, Kruskal Wallis test followed by a
697 post hoc Dunn's test. **I-J.** Phase shifts in hours in response to a 60min light pulse at indicated times
698 (n ≥ 26). Phase difference plotted as means ± SEM of differences from DD3-5. Same control flies
699 are plotted in I and J.

700

701 **Fig. 3: PDF from sLNvs maintains wakefulness under constant darkness. A**. Representative
702 images of sLNvs (top) and lLNvs (bottom) stained for TIM and PDF at ZT18. TIM labels all clock
703 neurons. There is loss of PDF staining in cells expressing both *UAS-Cas9* and UAS-3X-guides
704 against *Pdf (UAS-Pdf-g)*. Scale bar represents 10µm. **B**. Quantification of PDF staining intensity
705 from sLNv (top) and lLNv (bottom) neurons represented with boxplots, n ≥ 36 cells from at least
706 11 hemibrains per genotype. Letters represent statistically distinct groups; p<0.001, Kruskal
707 Wallis test followed by a post hoc Dunn's test. **C-E**. Sleep plots representing average sleep of flies
708 from DD1-4 in 30-minute bins. *UAS-Cas9* alone control is indicated in dark gray, *UAS-Pdf-g* alone
709 control in light gray whereas the experimental genotype expressing both is represented by color
710 indicated above the plots. **F-H**. Total sleep duration in a day for individual flies quantified (from
711 DD1-4) represented by a boxplot, n ≥ 55 per genotype from at least two independent experiments.
712 Letters represent statistically distinct groups, p<0.01; Kruskal Wallis test followed by a post hoc
713 Dunn's test. **I-K**. P-wake over a 24-hour period for individual flies quantified (from DD1-4)
714 represented by a boxplot, letters represent statistically distinct groups; p<0.001, Kruskal Wallis
715 test followed by a post hoc Dunn's test.
716
717 **Fig. 4: Adult-specific loss of PDF using an inducible Cas9 system results in loss of rhythmicity**
718 **and increased sleep. A**. Representative images of sLNvs stained for GFP, mRFP and PDF. 2
719 weeks post heat shock, there is loss of PDF staining in cells expressing both *UAS-Cas9* and *UAS-*
720 *Pdf-g*. In about 60% of the hemibrains analyzed, PDF staining was lost from all sLNvs, whereas
721 in the remaining 40% hemibrains, some mosaicism was observed as PDF staining was unchanged
722 in 1-2 sLNvs. Scale bar represents 10µm. **B**. Quantification of PDF staining intensity from sLNvs
723 represented with boxplots, n ≥ 39 cells from at least 12 hemibrains per genotype/condition. There
724 is a significant effect of both variables on the staining intensity and a significant interaction when
725 CRISPR reagents for inducible CRISPR for *Pdf* were combined with 3X heat shock (Two-way
726 ANOVA; *** Interaction p<0.001). **C**. Actograms represent double-plotted average activity of flies
727 from an experiment across multiple days. Yellow panel indicates lights ON. Panels in dotted boxes
728 indicate heat-shocked flies. **D**. Rhythmicity Index for individual flies quantified (from DD2-7)
729 represented by a boxplot, n ≥ 29 per genotype. There is a significant effect of both variables on
730 rhythmicity and a significant interaction when CRISPR reagents for inducible CRISPR for *Pdf*
731 were combined with 3X heat shock (Two-way ANOVA; *** Interaction p<0.001). **E**. Total sleep

732 duration in a day for individual flies quantified for DD1-4 represented by a boxplot. For the group
733 expressing both *UAS-Cas9* and *UAS-Pdf-g* with heat-shock, only data from the arrhythmic flies
734 are shown and used for statistics (indicated by AR). Also see Fig. S5D. There is a significant effect
735 of both variables on sleep duration and a significant interaction when CRISPR reagents for
736 inducible CRISPR for *Pdf* were combined with 3X heat shock (Two-way ANOVA; *** Interaction
737 p<0.001). **F**. p-wake over a 24-hour period for individual flies quantified (from DD1-4)
738 represented by a boxplot. For the group expressing both *UAS-Cas9* and *UAS-Pdf-g* with heat-
739 shock, only data from the arrhythmic flies are shown and used for statistics (indicated by AR).
740 Also see Fig. S5D. Only heat-shock had a significant effect on p-wake and there was no interaction
741 between the variables (Two-way ANOVA; N.I. = No Interaction, p=0.31).
742

743 **Fig. 5: Adult-specific loss of PDF with AGES leads to loss of rhythmicity and wakefulness.**
744 **A**. Representative images of sLNvs stained for mRFP and PDF. Upon feeding 10mM auxin for 2
745 weeks, there is loss of PDF staining in cells expressing both *UAS-Cas9* and *UAS-Pdf-g*. Scale bar
746 represents 10µm. **B**. Quantification of PDF staining intensity from sLNvs is represented with
747 boxplots, n ≥ 39 cells from at least 11 hemibrains per genotype/condition. There is a significant
748 effect of both variables on PDF staining intensity and a significant interaction when AGES and
749 CRISPR reagents for *Pdf* were combined with auxin feeding (Two-way ANOVA; *** Interaction
750 p<0.001). **C**. Actograms represent double-plotted average activity of flies from an experiment
751 across multiple days. Yellow panels indicate lights ON. Panels in dotted boxes indicate auxin
752 feeding. **D**. Rhythmicity Index for individual flies quantified (from DD2-7) represented by a
753 boxplot, n ≥ 31 per genotype. There is a significant effect of both variables on rhythmicity and a
754 significant interaction when AGES and CRISPR reagents for *Pdf* were combined with auxin
755 feeding (Two-way ANOVA; *** Interaction p<0.001). **E**. Total sleep duration in a day for
756 individual flies quantified (from DD1-4) represented by a boxplot. There is a significant effect of
757 both variables on sleep duration and a significant interaction when AGES and CRISPR reagents
758 for *Pdf* were combined with auxin feeding (Two-way ANOVA; *** Interaction p<0.001). **F**. p-
759 wake over a 24-hour period for individual flies quantified (from DD1-4) represented by a boxplot.
760 There is a significant effect of both variables on p-wake and a significant interaction when AGES
761 and CRISPR reagents for *Pdf* were combined with auxin feeding (Two-way ANOVA; ***
762 Interaction p<0.001). **G-I**. Rhythmicity Index for individual flies quantified (from DD2-6)

763 represented by a boxplot, $n \geq 30$ per genotype. Flies of the indicated genotypes were fed auxin for
764 either 2-, 4- or 7-days and compared with flies that were fed no auxin, or with flies with
765 mutagenesis throughout development (NO AGES). Letters represent statistically distinct groups;,
766 Kruskal Wallis test followed by a post hoc Dunn's test, $p<0.003$.
767

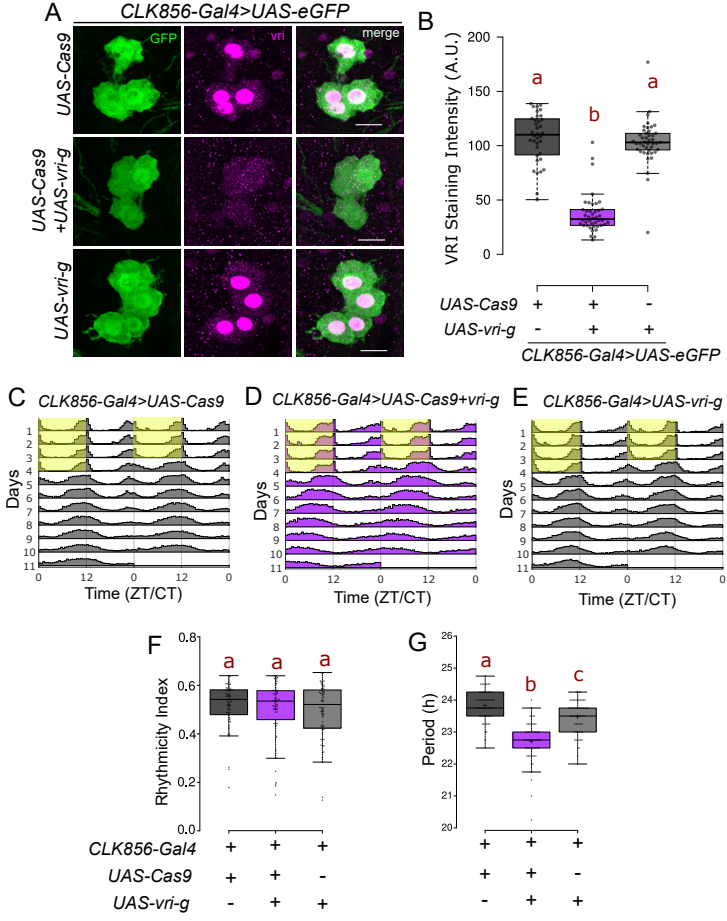
A
CLK856-Gal4>UAS-eGFP
GFP
vri
merge
UAS-Cas9
UAS-Cas9 +UAS-vri-g
UAS-vri-g
B
VRI Staining Intensity (A.U.)
200
150
100
50
0
a
b
a
UAS-Cas9 + + -
UAS-vri-g - + +
CLK856-Gal4>UAS-eGFP
C
CLK856-Gal4>UAS-Cas9
D
CLK856-Gal4>UAS-Cas9+vri-g
E
CLK856-Gal4>UAS-vri-g
Days
Time (ZT/CT)
F
Rhythmicity Index
0.8
0.6
0.4
0.2
0.0
a
a
a
G
Period (h)
26
25
24
23
22
21
20
a
b
c
CLK856-Gal4 + + +
UAS-Cas9 + + -
UAS-vri-g - + +

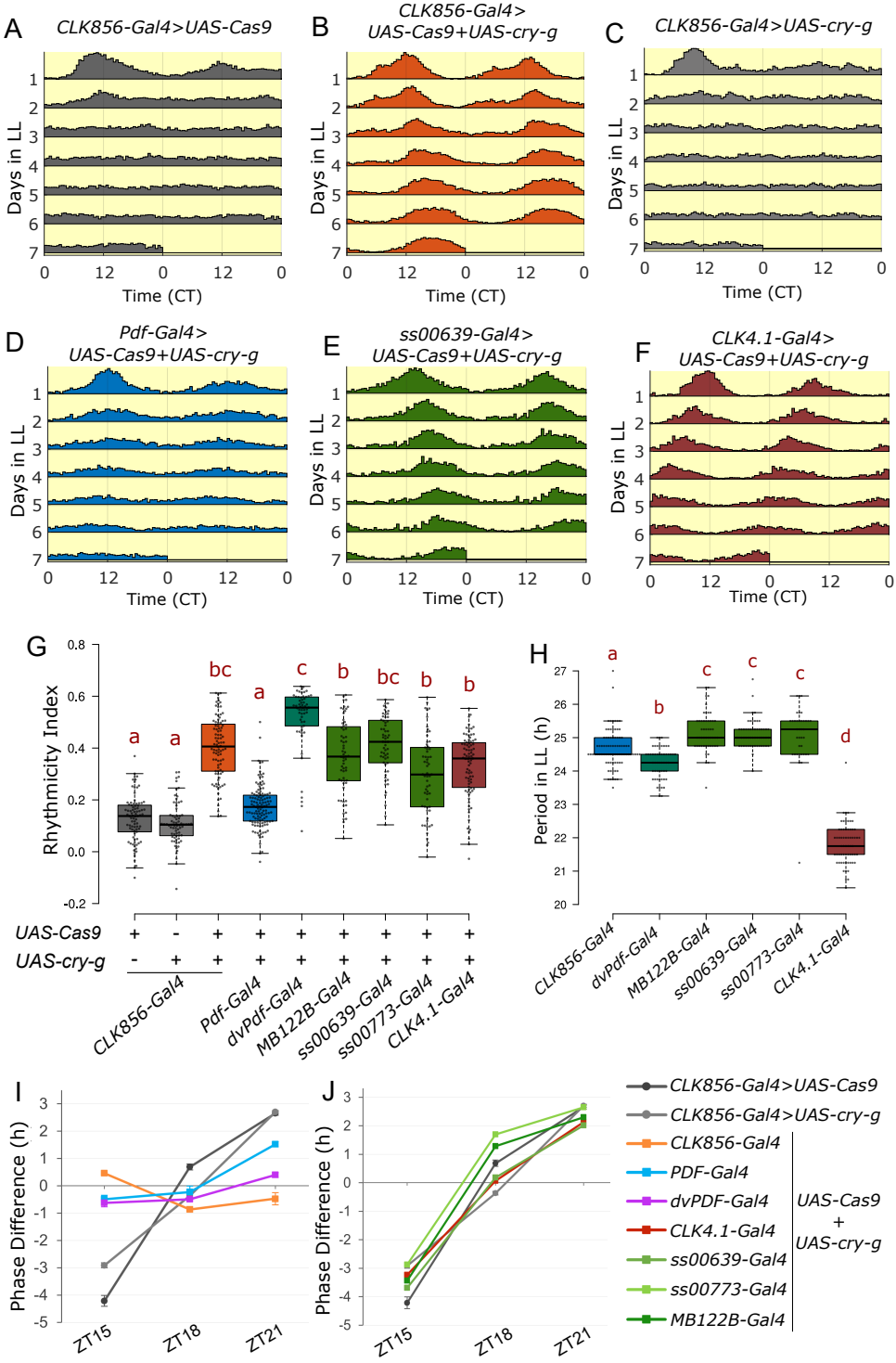
A
CLK856-Gal4>UAS-Cas9
B
CLK856-Gal4>
UAS-Cas9+UAS-cry-g
C
CLK856-Gal4>UAS-cry-g
D
Pdf-Gal4>
UAS-Cas9+UAS-cry-g
E
ss00639-Gal4>
UAS-Cas9+UAS-cry-g
F
CLK4.1-Gal4>
UAS-Cas9+UAS-cry-g
Days in LL
Time (CT)
G
Rhythmicity Index
H
Period in LL (h)
UAS-Cas9
UAS-cry-g
CLK856-Gal4
Pdf-Gal4
dvPdf-Gal4
MB122B-Gal4
ss00639-Gal4
ss00773-Gal4
CLK4.1-Gal4
I
J
Phase Difference (h)
ZT15
ZT18
ZT21
CLK856-Gal4>UAS-Cas9
CLK856-Gal4>UAS-cry-g
CLK856-Gal4
PDF-Gal4
dvPDF-Gal4
CLK4.1-Gal4
ss00639-Gal4
ss00773-Gal4
MB122B-Gal4
UAS-Cas9
+
UAS-cry-g

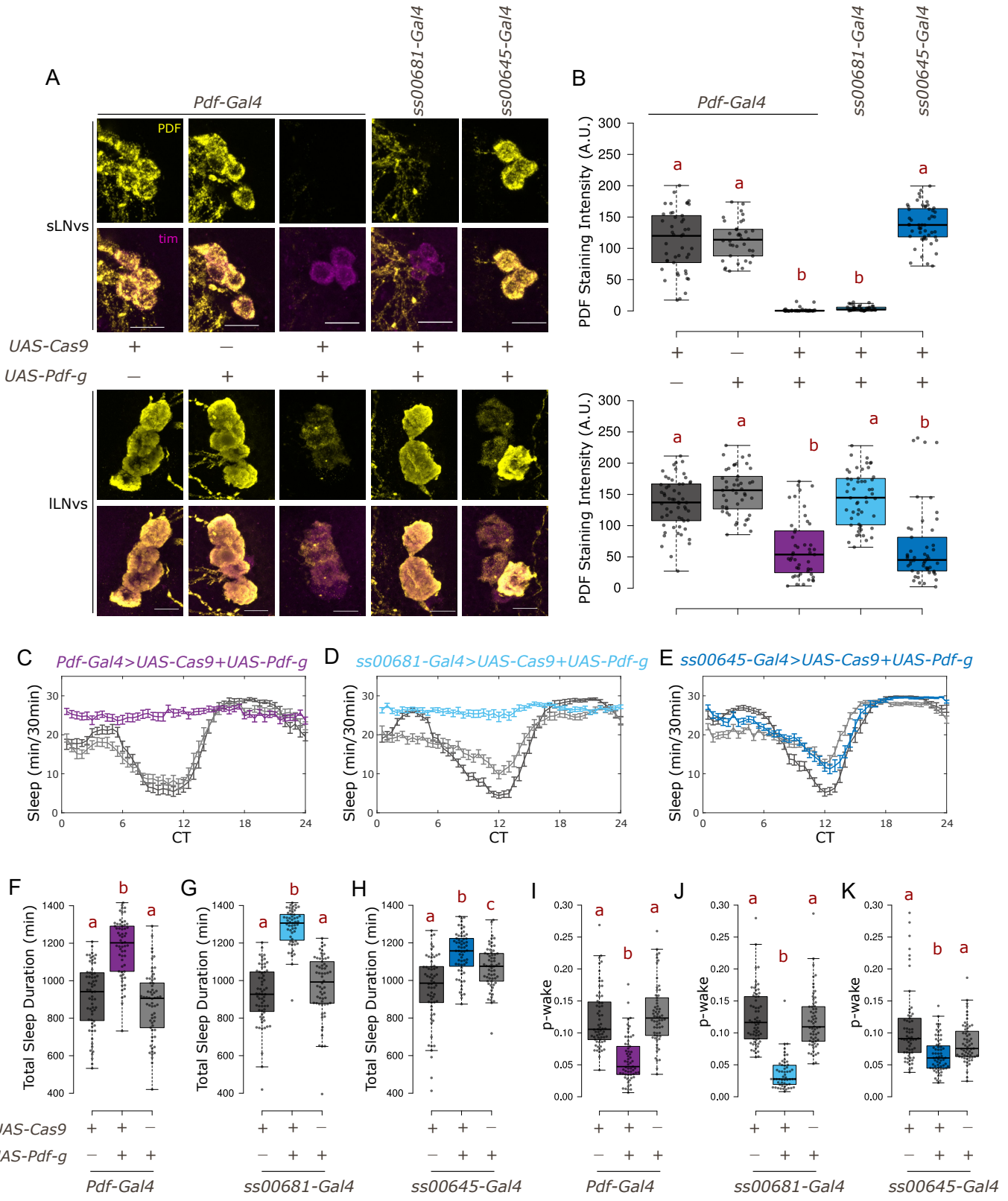
A
Pdf-Gal4
ss00681-Gal4
ss00645-Gal4
PDF
tim
sLNvs
lLNvs
UAS-Cas9
UAS-Pdf-g
B
PDF Staining Intensity (A.U.)
C
Pdf-Gal4>UAS-Cas9+UAS-Pdf-g
D
ss00681-Gal4>UAS-Cas9+UAS-Pdf-g
E
ss00645-Gal4>UAS-Cas9+UAS-Pdf-g
Sleep (min/30min)
CT
F
G
H
I
J
K
Total Sleep Duration (min)
p-wake

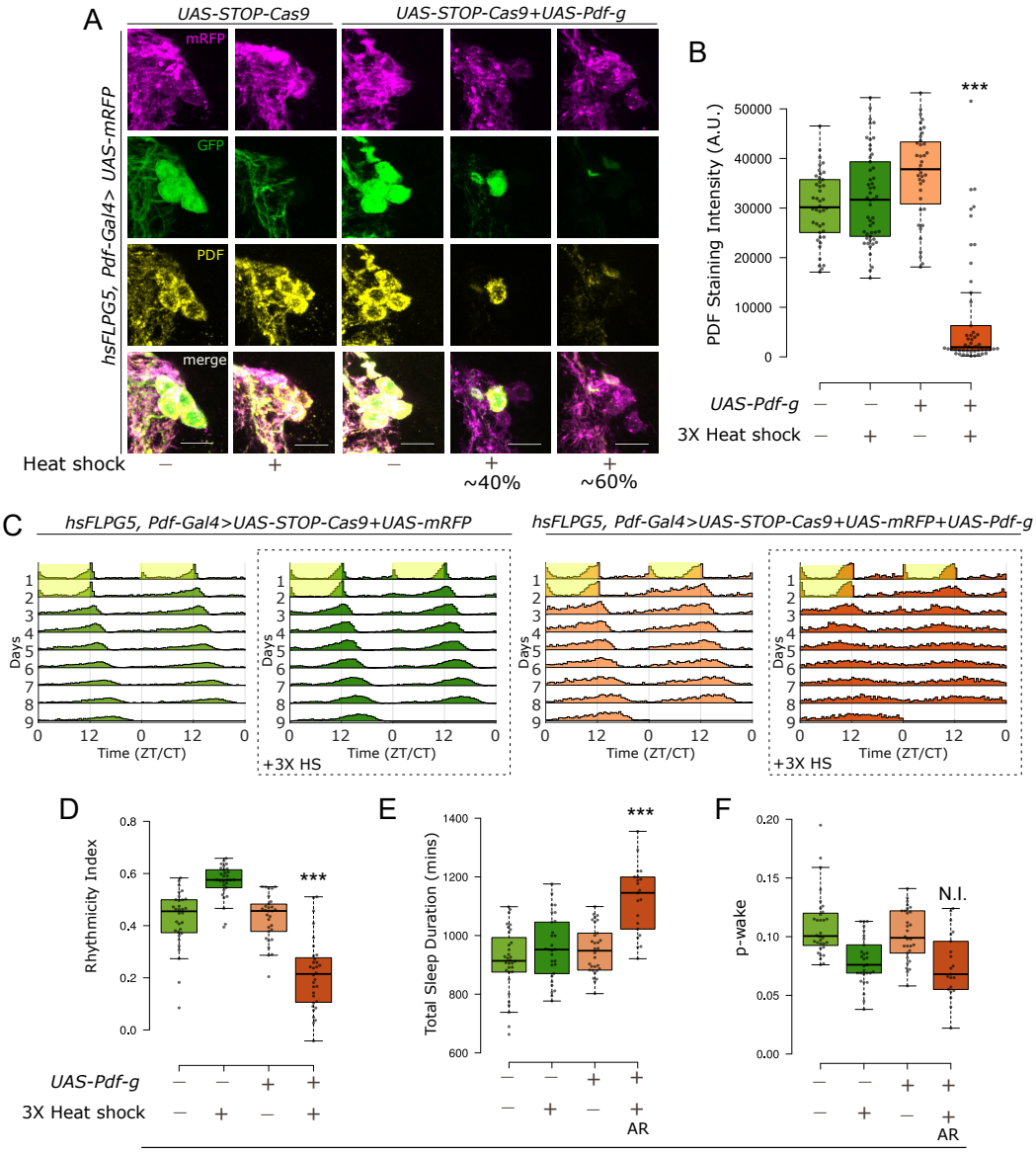
A
UAS-STOP-Cas9
UAS-STOP-Cas9+UAS-Pdf-g
hsFLPG5, Pdf-Gal4> UAS-mRFP
mRFP
GFP
PDF
merge
Heat shock
~40%
~60%
B
PDF Staining Intensity (A.U.)
***
UAS-Pdf-g
3X Heat shock
C
hsFLPG5, Pdf-Gal4>UAS-STOP-Cas9+UAS-mRFP
hsFLPG5, Pdf-Gal4>UAS-STOP-Cas9+UAS-mRFP+UAS-Pdf-g
Days
Time (ZT/CT)
+3X HS
D
Rhythmicity Index
E
Total Sleep Duration (mins)
AR
F
p-wake
N.I.
hsFLPG5, Pdf-Gal4>UAS-STOP-Cas9+UAS-mRFP

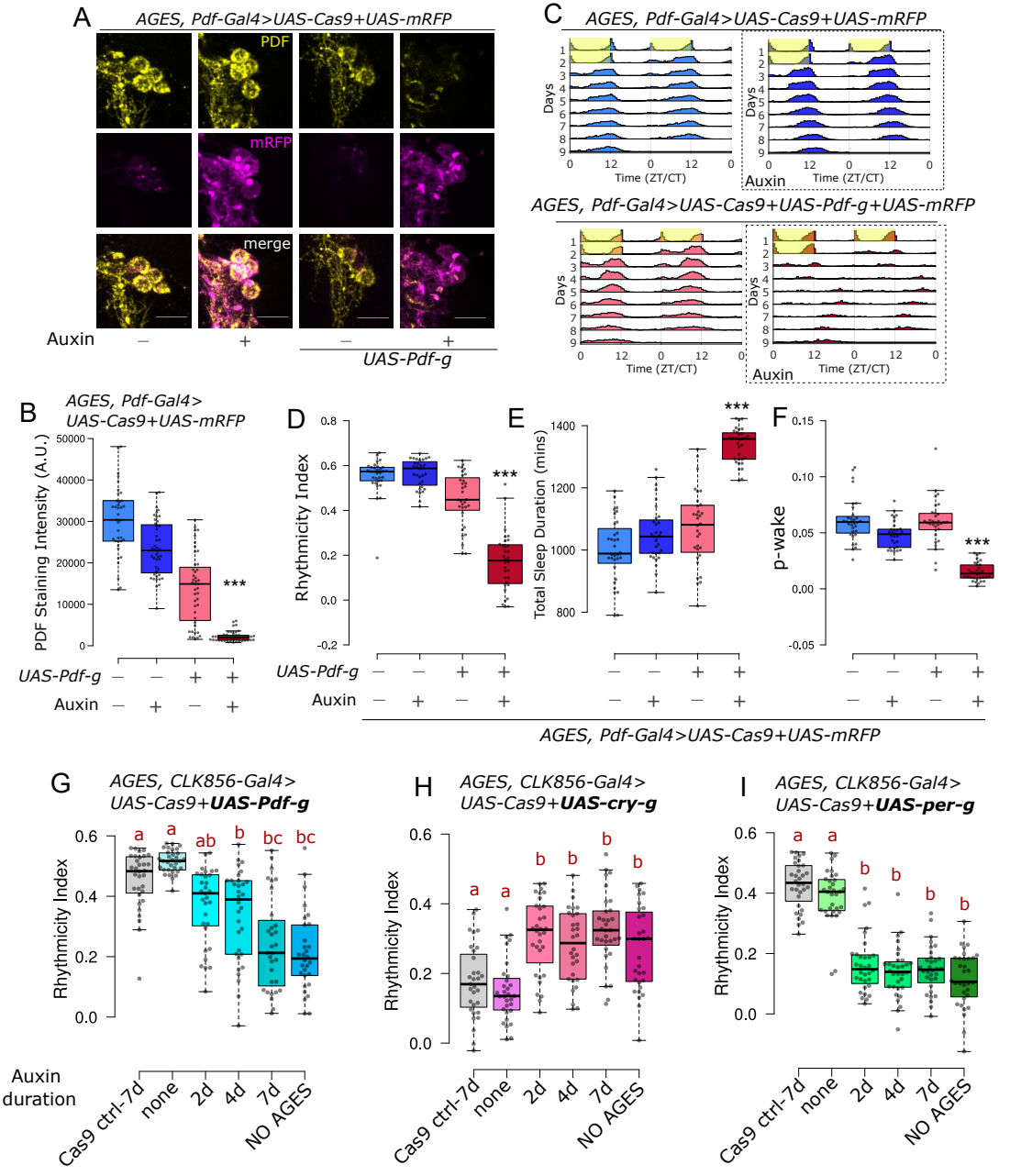
A
AGES, Pdf-Gal4>UAS-Cas9+UAS-mRFP
PDF
mRFP
merge
Auxin
UAS-Pdf-g
C
AGES, Pdf-Gal4>UAS-Cas9+UAS-mRFP
Days
Time (ZT/CT)
Auxin
AGES, Pdf-Gal4>UAS-Cas9+UAS-Pdf-g+UAS-mRFP
B
AGES, Pdf-Gal4>
UAS-Cas9+UAS-mRFP
PDF Staining Intensity (A.U.)
D
Rhythmicity Index
E
Total Sleep Duration (mins)
F
p-wake
AGES, Pdf-Gal4>UAS-Cas9+UAS-mRFP
G
AGES, CLK856-Gal4>
UAS-Cas9+UAS-Pdf-g
H
AGES, CLK856-Gal4>
UAS-Cas9+UAS-cry-g
I
AGES, CLK856-Gal4>
UAS-Cas9+UAS-per-g
Auxin duration
Cas9 ctrl-7d
none
2d
4d
7d
NO AGES

Supporting Information for

Dissecting neuron-specific functions of circadian genes using modified cell-specific CRISPR approaches.

Shlesha Richhariya[1], Daniel Shin[1], Jasmine Quynh Le[1] and Michael Rosbash[1]*

[1]Howard Hughes Medical Institute, Brandeis University, Waltham, MA 02454

*Correspondence – rosbash@brandeis.edu

This PDF file includes:

Supporting Materials and Methods
Figures S1 to S8
Tables S1 to S4
Legend for Dataset S1
SI References

Other supporting materials for this manuscript include the following:

Dataset S1

SI Materials and Methods:

Generation of Fly Lines

To generate lines expressing 3X-guides under UAS-control, we used previously described protocols (Port and Bullock, 2016; Schlichting et al., 2019). Briefly, gRNAs specific to the target genes were identified using the CRISPR Optimal Target Finder tool (Gratz et al., 2014). These gRNA sequences were incorporated into the tRNA backbone using 2 PCR reactions, primers for which are listed in supplementary Table S4. The PCR products were assembled into the UASpCFD6 vector (Addgene #73915) digested with BbsI-HF enzyme (NEB) using Gibson assembly. Sequence verified plasmids were injected into the attP2 site on the third chromosome by Rainbow Transgenic Flies Inc (Camarillo, CA, USA). Positive transformants were screened for by red eye color based on the miniwhite marker.

Locomotor Activity and Sleep Behavior

Circadian rhythmicity and sleep analysis was performed using the 2020 version of Sleep and Circadian Analysis MATLAB Program (SCAMP) developed by Christopher G. Vecsey (Donelson et al., 2012). For period analysis, only rhythmic flies (Rhythmicity Index > 0.25) were used, apart from PDF perturbations in Fig. S6 and Table S2, where flies with Rhythmicity Index >0.2 were defined as rhythmic to look for residual short period rhythms in partially arrhythmic flies. E-peak timing was calculated as the highest point in bins from ZT6.5-ZT10.5 of average activity in 30 min bins exported from SCAMP. Sleep structure analysis for p-wake and p-doze (Wiggin et al., 2020) was also performed using this new version of SCAMP.

For phase shift experiments about 2-week-old males flies were entrained to LD for at least 3 days and on the last night of LD, 1 hour light pulse (500 lux) was delivered either at ZT15, ZT18 or ZT21. For one set of flies, no light pulse was given, and these were used as controls to calculate phase shift using the SCAMP program. Average shifts from days 3-5 are reported.

Heat shock for inducible Cas9

For experiments with the inducible Cas9 system, 2-5 days old male flies of the appropriate genotype were heat shocked on 3 consecutive days. The first heat shock was 25 mins, and the two subsequent ones were 40 mins each. Heat shock was delivered by placing flies in an empty food vial and submerging the vial in a water bath set at 37°C. Flies were removed promptly and allowed to recover briefly at room temperature before being transferred to a fresh vial with standard cornmeal food. Once the flies recovered completely, the flies were placed in an incubator set to 25°C. Flies were aged for 2 weeks from the day of the first heat shock before loading them in behavior experiments. Control flies were collected at the same time and aged simultaneously but without the heat shock.

Auxin feeding for adult-specific behavior with AGES

For AGES experiments, 2-5 days old male flies were fed Instant *Drosophila* Medium (Formula 424®, Carolina) reconstituted either in 10mM Auxin (GK2088, Glentham Life Sciences) or distilled water (for controls). Flies were fed this food for about 2 weeks before loading them in behavior tubes with standard behavior food (4% sucrose and 2% agar). Since CRISPR based mutagenesis irreversibly alters the DNA in the cells of interest, we used standard behavior food for behavior analysis post auxin feeding to make experiments simpler. For AGES time course, 0-2 day old male flies expressing gRNA and Cas9 with CLK856 Gal4 and AGES were collected and divided into 4 groups – No auxin, auxin fed for 2days, 4 days and 7 days. Flies were fed auxin for the indicated duration, starting later for shorter durations, and then tested for behavior on standard behavior food.

Immunohistochemistry and Image Analysis

Whole flies of the same genotype and age as the behavior experiment cohort were fixed at ZT18-19 in 4% paraformaldehyde in PBS with 0.4% Triton X-100 for 2 hours and 30 minutes at room temperature. Tubes were wrapped in tin foil to protect them from light while rotating on a shaker. Flies were then washed three times (10 minutes each) with 0.4% PBST before dissecting the

brain. Dissected brains were washed and blocked with 10% Normal Goat Serum (NGS; Jackson labs) in 0.4% PBST (blocking buffer) for 2 hours at room temperature or at 4°C overnight. The following primary antibodies were used diluted in blocking buffer– chicken anti-GFP (Abcam ab13970; 1:1000), mouse anti-PDF (DSHB-PDF C7; 1:1000), guinea pig anti-VRI (gift of Paul Hardin; 1:3000 (Glossop et al., 2003)), rat anti-TIM (Rosbash lab; 1:250, (Ma et al., 2021)), rabbit anti-PER (Rosbash lab, 1:1000, (Ma et al., 2021)), rabbit anti-dsRed (Takara Bio- 632393; 1:300) and rat anti-RFP (Proteintech-5f8; 1:1000). Primary antibody was incubated for 24-36 hours at 4°C. The brains were then washed three times (30 minutes each) in 0.4% PBST, and corresponding secondary antibodies were used at a 1:500 dilution in blocking buffer and incubated at 4°C overnight. Brains were again washed three times (30 minutes each) in 0.4% PBS, mounted in VectaShield mounting medium (Vector Laboratories).

For CRY immunostaining, flies were kept in constant darkness for several days to allow accumulation and detection of CRY as described earlier (Yoshii et al., 2008). Flies were fixed at CT0-1 (DD4) in dark conditions. The rat anti-CRY antisera (Emery et al., 1998) were incubated with fixed heads of the null mutants, cry^{01} (Dolezelova et al., 2007) to reduce background staining. This primary rat anti-CRY antibody was used at 1:200.

Images were acquired using Leica Stellaris 8 confocal microscope equipped with a white light laser. Images for one set of experiments were acquired using the Leica SP5 confocal microscope. For each experiment, the laser settings were kept constant across genotypes. Either 20X air objective or a 40X oil objective (for image quantification) with NA of 1.43 was used. Image analysis was performed with Fiji (Schindelin et al., 2012) using the Time Analyzer V3 plugin to mark ROIs across channels and measure intensity of the PDF channel. Background intensity for a z-stack was measured from three random background regions, averaged, and subtracted from each ROI.

Data representation and Statistical Analysis

Some of the figure panels (Fig. S5A, S7A and S8A) were created using BioRender. Boxplots were generated using BoxPlotR (Spitzer et al., 2014). For all boxplots, center lines show the medians; box limits indicate the 25th and 75th percentiles as determined by R software; whiskers extend 1.5 times the interquartile range from the 25th and 75th percentiles, outliers are represented by dots. Source data for all figures are included in SI Dataset 1. Statistical tests performed are described in the figure legends. All statistical tests were performed using the free online tool Statistics Kingdom https://www.statskingdom.com/index.html

Supplementary Figures

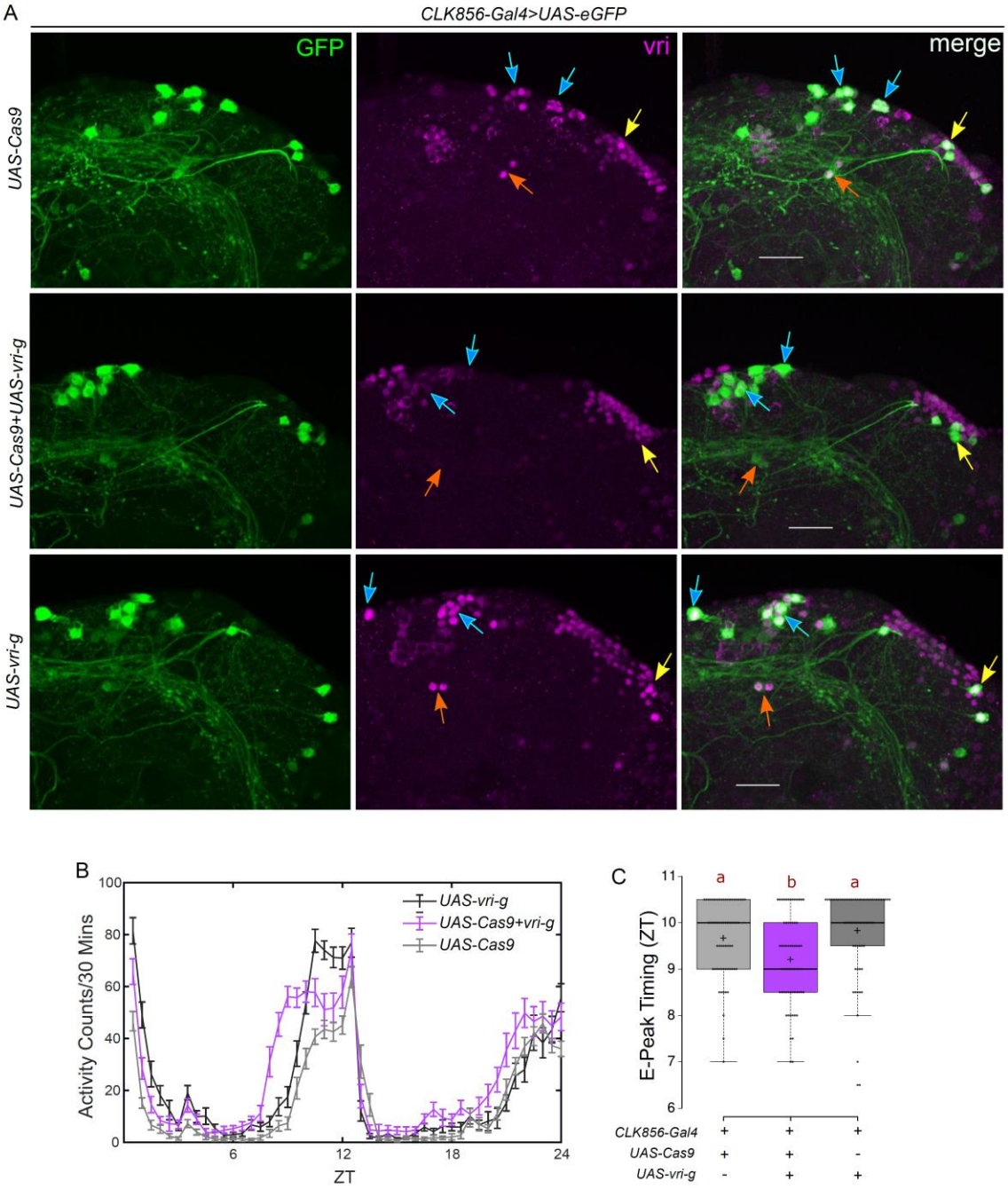

Fig. S1: Loss of VRI from clock neurons leads to an advanced evening peak. A. Representative images of the dorsal circadian neurons stained for GFP and VRI at ZT19. There is loss of VRI staining in cells expressing *CLK856-Gal4* (marked by GFP) but no loss in GFP-negative cells. Arrows point to examples of Gal4-positive DN1s (blue), DN2s (red) and DN3s (yellow) in the indicated genotypes. Scale bar represents 20µm. **B**. Average activity

counts for flies in an experiment plotted as a function of time. Flies with loss of VRI in *CLK856-Gal4* labelled neurons showed an advanced evening peak. **C**. Quantification of the evening peak (E-peak) timing from individual flies, $n \geq 62$ per genotype from at least two independent experiments. Letters represent statistically distinct groups; $p<0.01$, Kruskal Wallis test followed by a post hoc Dunn's test.

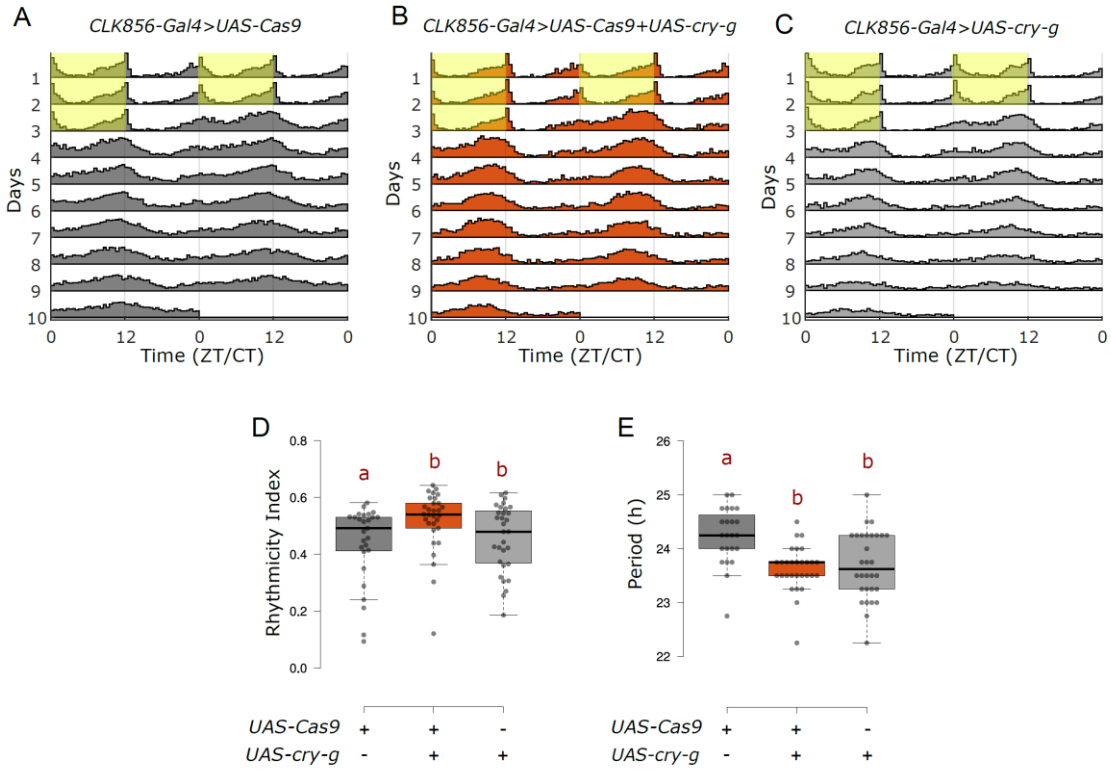

Fig. S2: CRY mutation in clock neurons does not affect circadian behavior under constant darkness. A-C. Actograms represent double-plotted average activity of flies from an experiment across multiple days. Yellow panels indicate lights ON. **D**. Rhythmicity Index for individual flies quantified for DD2-7 represented by a boxplot, n ≥ 27 per genotype, letters represent statistically distinct groups, p<0.01, Mann-Whitney U test post Kruskal Wallis ANOVA. **E**. Free running period under constant darkness for individual flies quantified for DD2-7 represented by a boxplot, letters represent statistically distinct groups; p<0.01, Kruskal Wallis test followed by a post hoc Dunn's test.

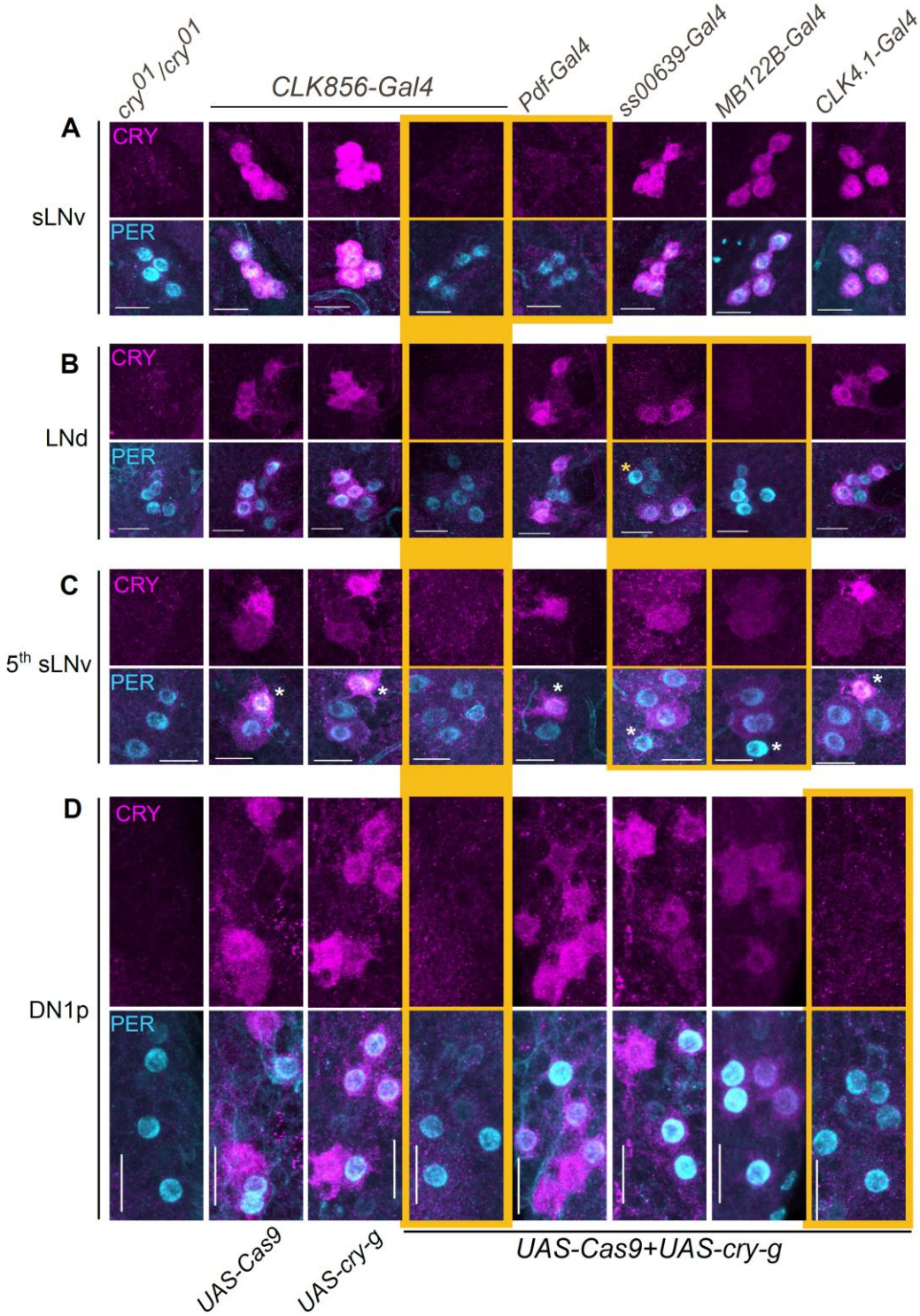

Fig. S3: CRISPR mediated cell specific mutagenesis of cry leads to cell-type specific loss of CRY-staining. Images from brains co-stained with CRY and PER, to label clock neurons at CT0-1 (DD4). In controls (columns 2 and 3), CRY staining is detected strongly in

the sLNvs, 3 of the 6 LNds, the 5th sLNv and a subset of the DN1ps whereas weakly in the lLNvs. CRY staining was absent from all clock neurons in the cry null mutant (*cry^{01}/cry^{01}*; column 1). Similarly, CRISPR mediated knockout of CRY with *CLK856-Gal4* led to severely reduced CRY staining in all clock neurons (A-D; column 4), whereas CRISPR mutagenesis with specific Gal4s led to loss of CRY staining from specific neurons as described below. Panels where CRY staining is perturbed are highlighted in yellow. **A**. CRY staining in the sLNv neurons was perturbed only with *Pdf-Gal4.* **B**. CRY mutagenesis with *MB122B-Gal4* led to loss of CRY staining from all three LNds whereas that with *ss00639-Gal4* led to loss of CRY staining from only one LNd (marked by asterisk). **C.** In the 5th sLNv (marked by asterisk), CRY staining is lost with CRISPR mutagenesis in *MB122B-Gal4* and *ss00639-Gal4.* **D**. CRY staining in the DN1ps is lost only when expression is targeted with the *CLK4.1-Gal4.* Scale bars represent 10µm.

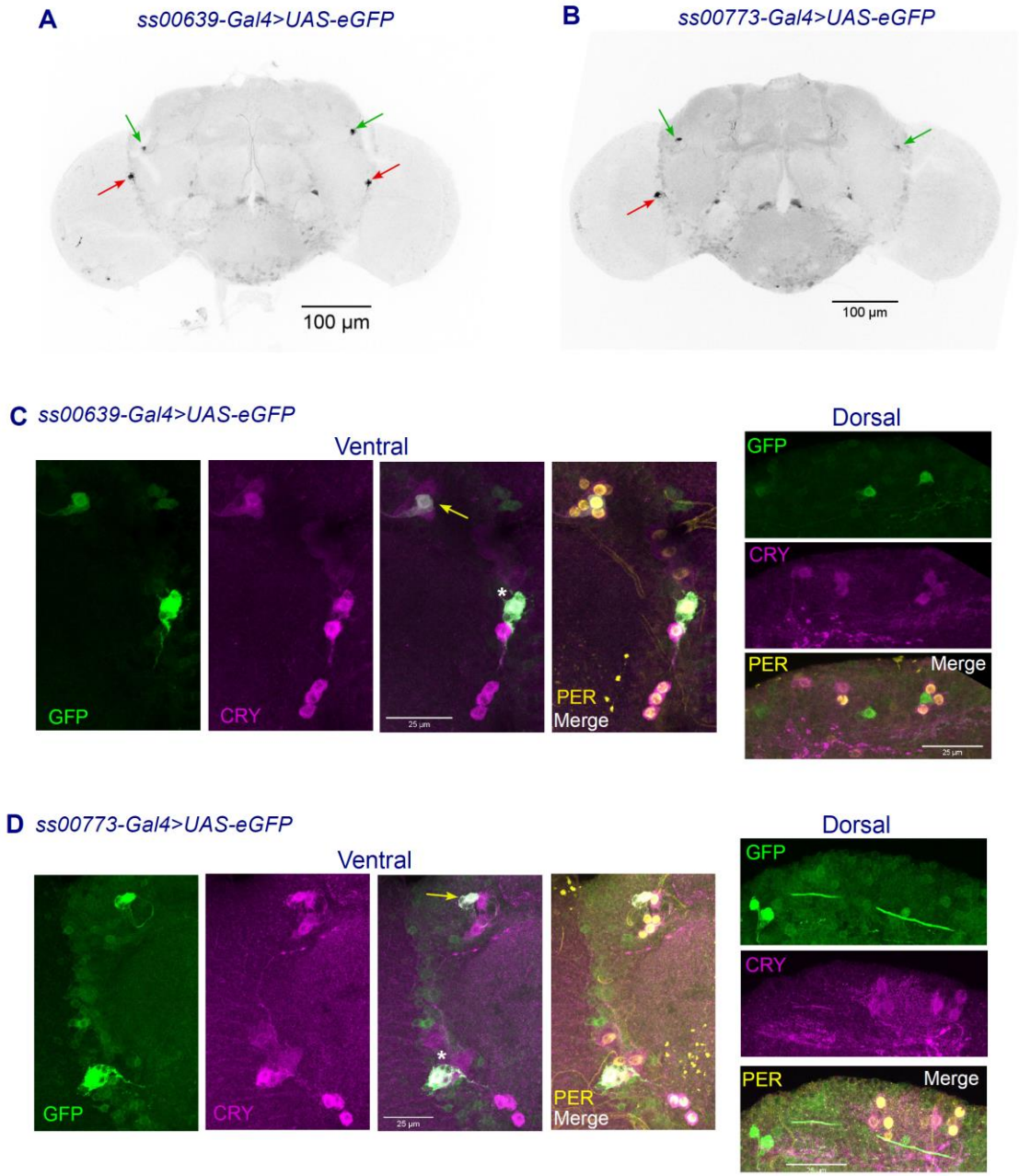

Fig. S4: Split-Gal4 drivers labelling a subset of evening cells. A-B: Full brain expression patterns of the two split-Gal4 drivers labelled by UAS-eGFP. **C-D:** Split-Gal4 lines co-stained with CRY and PERIOD (PER) to label clock neurons. Both split-Gal4s label the CRY and PER positive 5th sLNv (marked by asterisk) and one LNd (yellow arrow). In panels A-B, red arrows point to the 5th-sLNv and green arrows to an LNd neuron as identified by co-staining with clock

proteins in C-D. The *ss00639-Gal4* labels the 5th-sLNv + 1 LNd per hemisphere in all brains. The *ss00773-Gal4* also labels the 5th-sLNv + 1 LNd, but it does so more variably and labels about 2-4 of these clock cells per brain. Both Gal4s also label a few extra cells, *ss00773-Gal4* more so than *ss00639-Gal4,* but none of them are either PER or CRY positive.

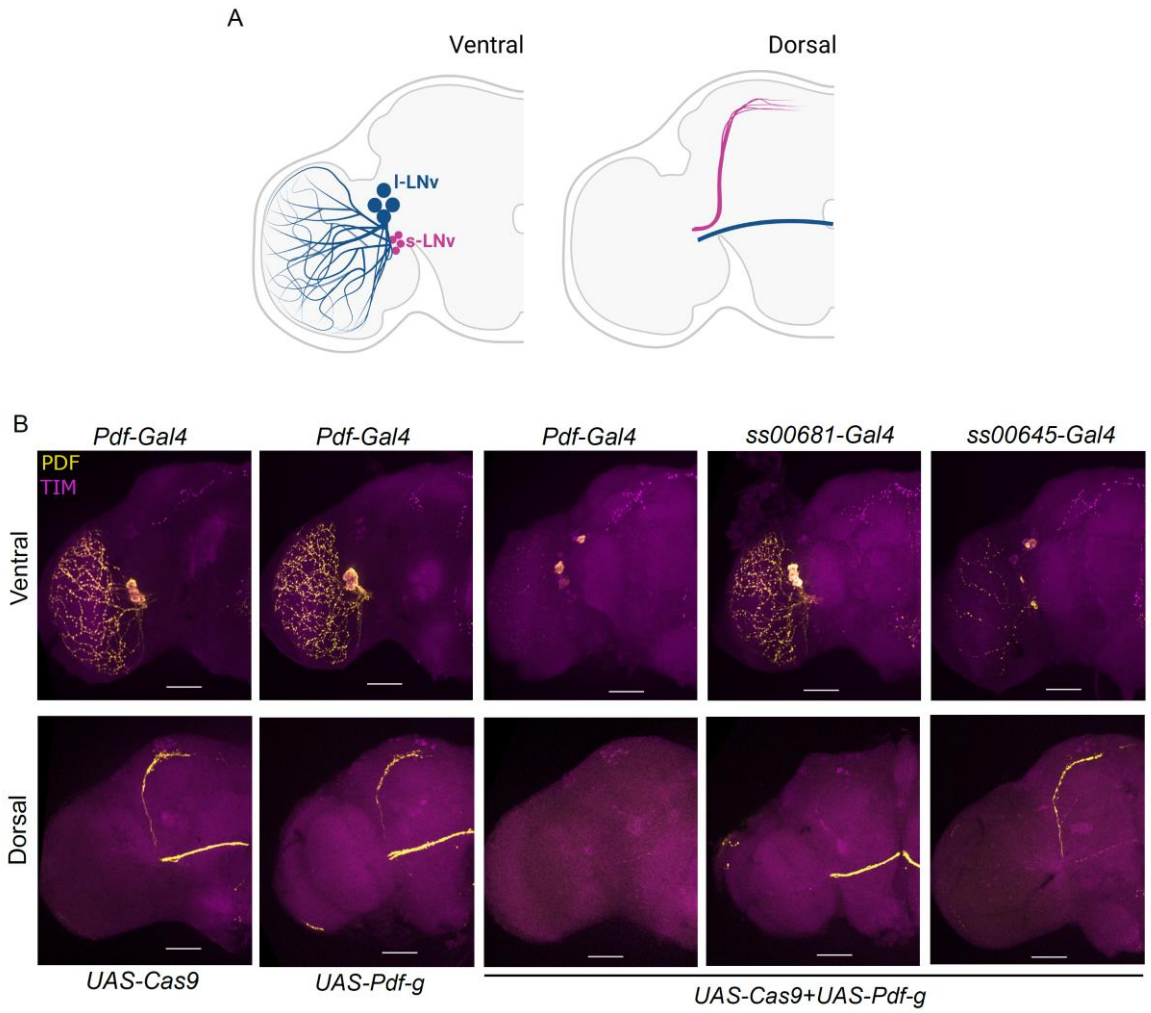

Fig. S5: CRISPR strategy successfully eliminates PDF staining from cell type-specific projections. A. Cartoon representation of the projection patterns of small (magenta) and large (blue) LNV neurons in the ventral and dorsal *Drosophila* brain. **B**. Representative images of hemibrains imaged from the ventral (top) or dorsal (bottom) side stained for PDF and TIM. For the dorsal panels, brightness-contrast was enhanced for the PDF channel equally across genotypes to confirm absence of PDF staining from the respective processes. Expression of both *UAS-Cas9* and *UAS-Pdf-g* with *Pdf-Gal4* leads to loss of all PDF staining from all PDF neurons. Expression with *ss00681-Gal4* that labels only the sLNvs leads to loss of PDF staining from their cell bodies and projections with no obvious effect on PDF staining in lLNvs.

Expression with *ss00645-Gal4* leads to loss of PDF staining in most projections of these neurons with no obvious effect on PDF staining in sLNvs.

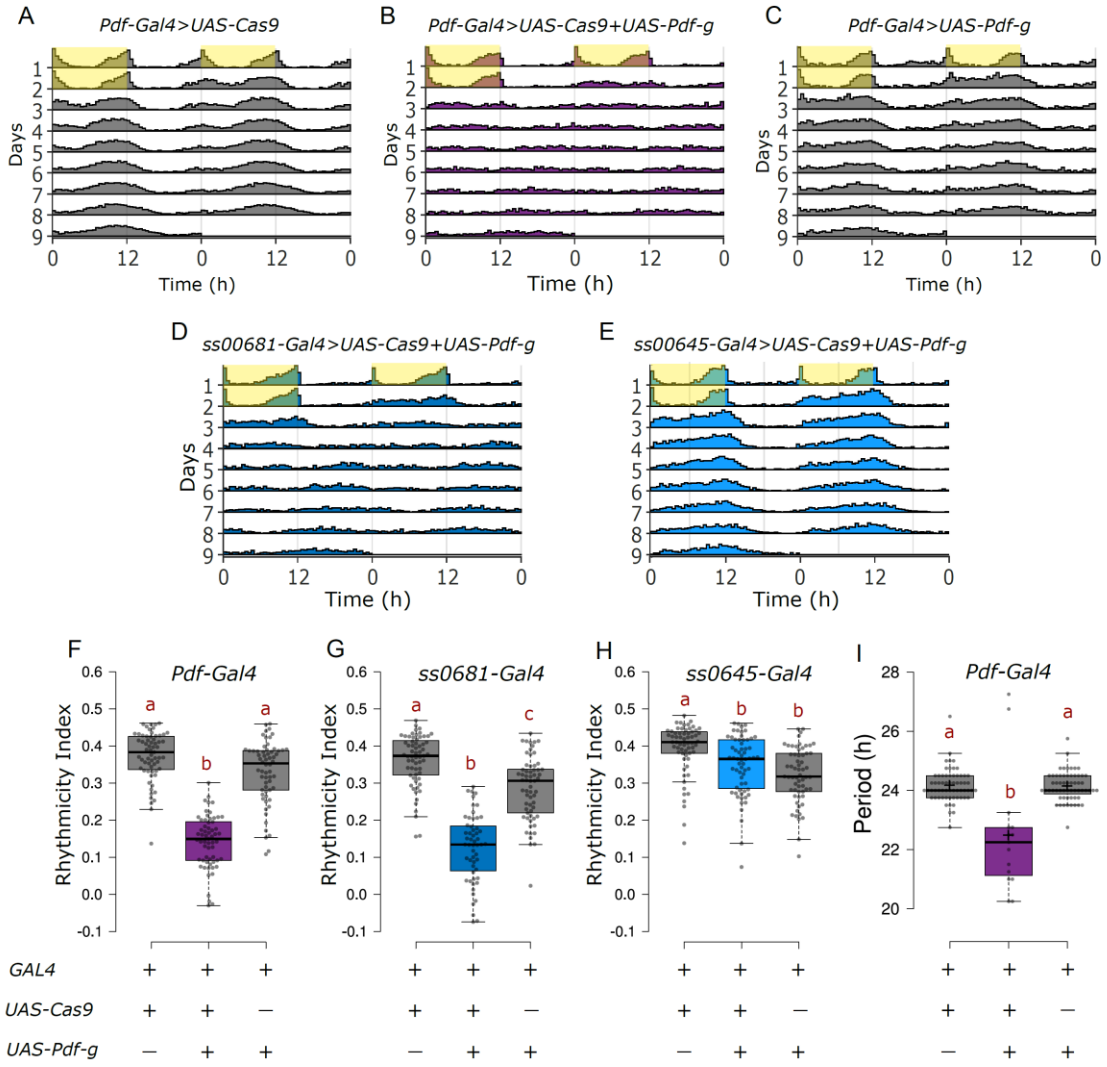

Fig. S6: Loss of PDF from sLNvs leads to loss of rhythmicity under constant darkness. **A-E**. Actograms represent double-plotted average activity of flies from an experiment across multiple days. Yellow panels indicate lights ON. **F-H**. Rhythmicity Index for individual flies quantified for DD1-4 represented by a boxplot, n ≥ 55 per genotype from at least two independent experiments, letters represent statistically distinct groups; p<0.01, Kruskal Wallis test followed by a post hoc Dunn's test. Loss of PDF from both sLNvs and lLNvs or from sLNvs alone causes arrhythmicity in constant darkness, whereas loss of PDF from lLNvs alone has no effect. **I.** Free running period for flies of the indicated genotypes, rhythmic flies (RI>0.2) with loss of PDF in PDF neurons have a shorter period.

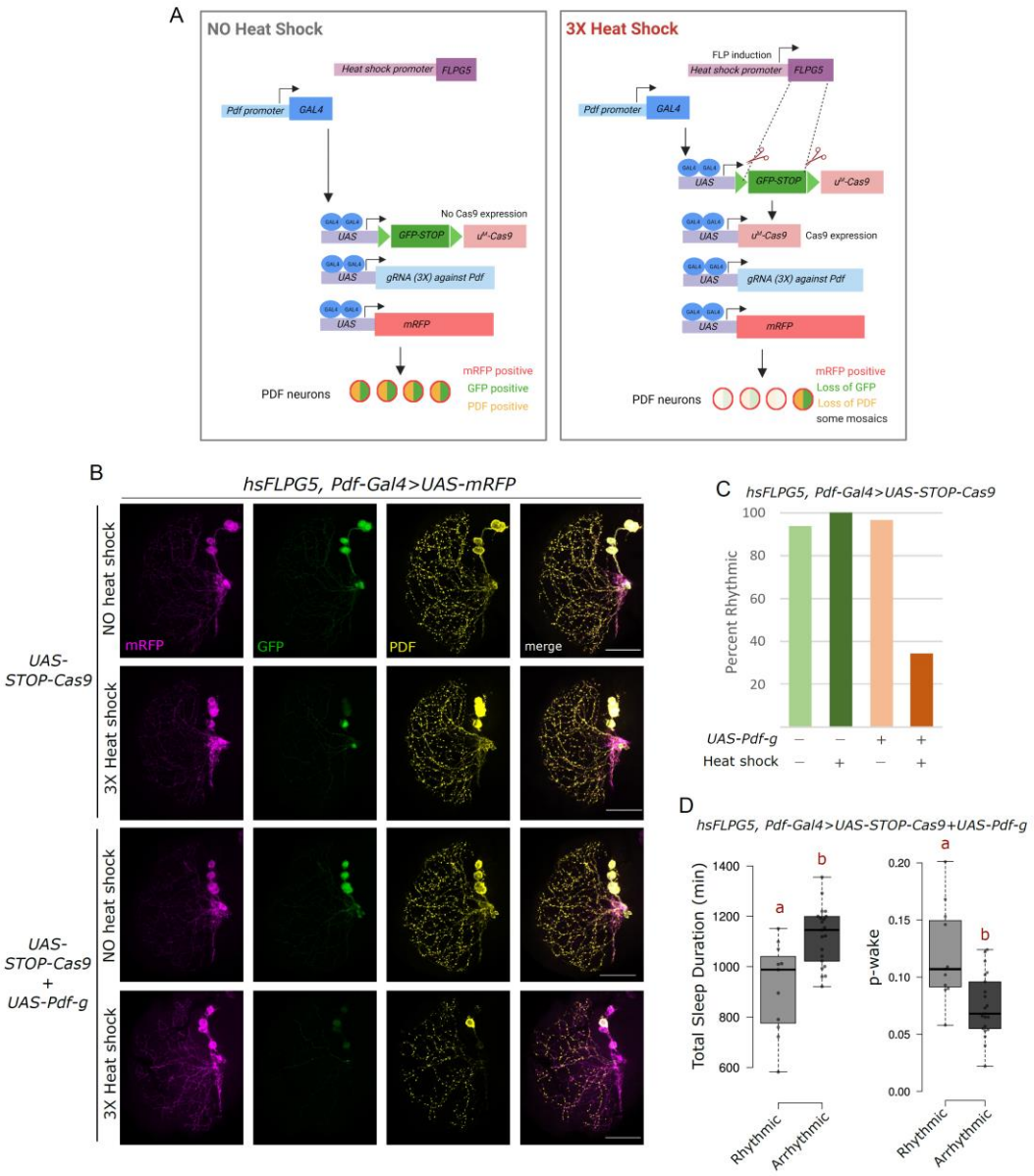

Fig. S7: The inducible-Cas9 systems is an effective tool for adult specific and cell type specific CRISPR mutagenesis despite some mosaics. A. Cartoon representation of the inducible Cas9 system (Port et. al., 2020) adapted to the adult-specific perturbation of PDF from PDF neurons. **B**. Representative images of the optic lobe ventral projections of the lLNvs. Scale bar represents 50µm. **C**. Plot indicating the percentage of flies rhythmic under the indicated conditions. **D**. Sleep parameters of flies expressing both *UAS-Cas9* and *UAS-Pdf-g* with heat-shock separated into rhythmic (RI>0.25) and arrhythmic (RI<0.25) categories, n=11 for rhythmic and 21 for arrhythmic. Arrhythmic flies have more sleep and a lower p-wake;

$p<0.01$, Mann Whitney U test. These rhythmic flies could be the result of the mosaicism, i.e., PDF expression in 1-2 sLNvs might be sufficient for quasi-normal circadian and sleep behavior.

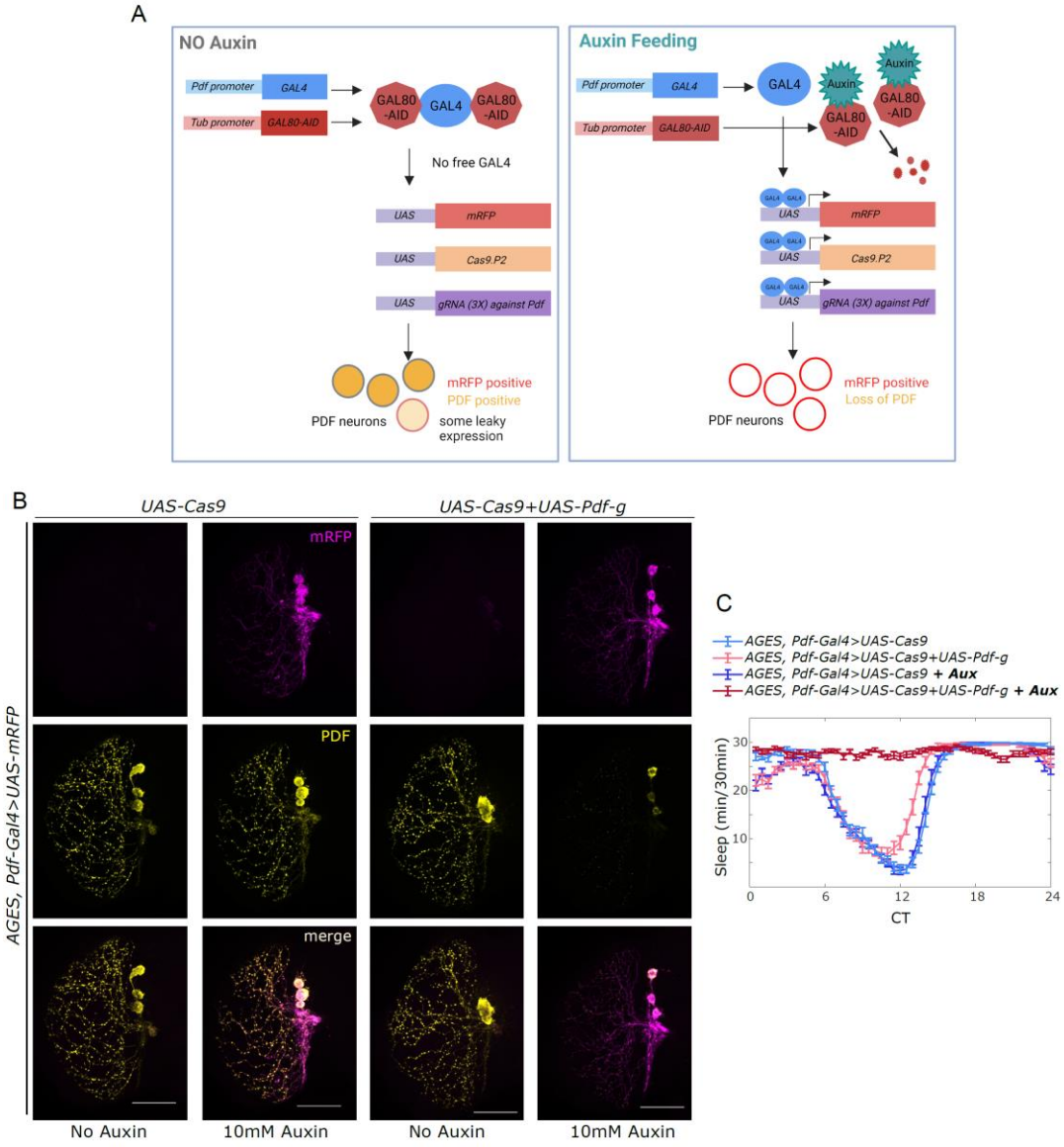

Fig. S8: AGES is mildly leaky, but still an effective tool for adult-specific, cell type-specific CRISPR mutagenesis. A. Cartoon representation of the AGES system (McClure et. al., 2022) adapted to the adult specific perturbation of PDF from PDF neurons. **B**. Representative images of the optic lobe ventral projections of the lLNvs. Scale bar represents 50µm. **C**. Sleep plot representing average sleep of flies from DD1-4 in 30-minute bins.

Supplementary Tables

Table S1: Summary of circadian behavior with cell type-specific CRY mutants in constant light.

Genotype	Cells labelled	n	Rhythmicity Index LL2-7 (Mean ± SEM)	%Rhythmic (RI>0.25)	Period (h) (Mean ± SEM)
CLK856-Gal4>UAS-Cas9	Most clock neurons (many DN3s missing)	85	0.13 ± 0.01	10.6	-
CLK856-Gal4>UAS-CRYg		72	0.11 ± 0.01	6.9	-
CLK856-Gal4>UAS-Cas9+UAS-CRYg		**92**	**0.40 ± 0.01**	**90.2**	**24.71 ± 0.07**
PDF-Gal4>UAS-Cas9	sLNvs+ lLNvs	118	0.10 ± 0.01	6.8	-
PDF-Gal4>UAS-CRYg		119	0.12 ± 0.01	5.0	-
PDF-Gal4>UAS-Cas9+UAS-CRYg		**121**	**0.17 ± 0.01**	**14.9**	-
dvPDF-Gal4>UAS-Cas9	sLNvs+ lLNvs+ 5th sLNv+ 1 CRY^{+} ITP^{+} LNd + 3 CRY^{-}LNds	56	0.14 ± 0.01	8.9	-
dvPDF-Gal4>UAS-CRYg		51	0.15 ± 0.01	9.8	-
dvPDF-Gal4>UAS-Cas9+UAS-CRYg		**58**	**0.52 ± 0.02**	**91.4**	**24.24 ± 0.06**
MB122B-Gal4>UAS-Cas9	5th sLNv + 1 CRY^{+}ITP^{+} + 2 CRY^{+} Trissin^{+} LNds	64	0.15 ± 0.01	9.4	-
MB122B--Gal4>UAS-CRYg		61	0.14 ± 0.01	3.3	-
MB122B-Gal4>UAS-Cas9+UAS-CRYg		**63**	**0.37 ± 0.02**	**79.4**	**25.08 ± 0.08**
ss00639-Gal4>UAS-Cas9	5th sLNv + 1 CRY^{+} LNd	64	0.14 ± 0.01	9.4	-
ss00639-Gal4>UAS-CRYg		58	0.15 ± 0.01	10.3	-
ss00639-Gal4>UAS-Cas9+UAS-CRYg		**60**	**0.41 ± 0.01**	**91.7**	**25.11 ± 0.06**
ss00773-Gal4>UAS-Cas9	5th sLNv + 1 CRY^{+} LNd	63	0.14 ± 0.01	4.8	-
ss00773-Gal4>UAS-CRYg		60	0.15 ± 0.01	8.3	-
ss00773-Gal4>UAS-Cas9+UAS-CRYg		**61**	**0.29 ± 0.02**	**60.7**	**25.06 ± 0.14**
CLK4.1-Gal4>UAS-Cas9	DN1p	72	0.12 ± 0.01	9.7	-
CLK4.1-Gal4>UAS-CRYg		69	0.13 ± 0.01	5.8	-
CLK4.1-Gal4>UAS-Cas9+UAS-CRYg		**83**	**0.33 ± 0.01**	**74.7**	**21.82 ± 0.08**

Table S2: Summary of circadian and sleep behavior upon loss of PDF from specific neurons.

Genotype	cells labelled	n	Percent Rhythmic (RI>0.2)	Rhythmicity Index (DD1-4)	Average total sleep per day(min)	Activity while awake	pwake	pdoze
				Mean ± SEM				
PDF-Gal4>UAS-Cas9	All sLNvs + lLNvs	63	98.4	0.37 ± 0.01	914 ± 22	1.62 ± 0.04	0.12 ± 0.006	0.37 ± 0.01
PDF-Gal4>UAS-PDFg		62	90.3	0.33 ± 0.01	873 ± 23	1.79 ± 0.05	0.13 ± 0.007	0.35 ± 0.01
PDF-Gal4>UAS-Cas9 + UAS-PDFg		**61**	**24.6**	**0.14 ± 0.01**	**1178 ± 19**	**2.52 ± 0.10**	**0.06 ± 0.005**	**0.40 ± 0.01**
ss00681-Gal4>UAS-Cas9	All sLNvs	63	96.8	0.36 ± 0.01	924 ± 19	1.81 ± 0.04	0.12 ± 0.006	0.38 ± 0.01
ss00681-Gal4>UAS-PDFg		62	83.9	0.29 ± 0.01	972 ± 21	2.17 ± 0.07	0.12 ± 0.006	0.42 ± 0.01
ss00681-Gal4>UAS-Cas9 + UAS-PDFg		**55**	**23.6**	**0.13 ± 0.01**	**1284 ± 13**	**2.57 ± 0.10**	**0.04 ± 0.003**	**0.44 ± 0.01**
ss00645-Gal4>UAS-Cas9	Variably 3-4 lLNvs per hemi-brain	62	96.8	0.39 ± 0.01	957 ± 23	1.79 ± 0.05	0.11 ± 0.008	0.34 ± 0.01
ss00645-Gal4>UAS-PDFg		61	96.7	0.32 ± 0.01	1068 ± 14	2.37 ± 0.10	0.08 ± 0.004	0.38 ± 0.01
ss00645-Gal4>UAS-Cas9 + UAS-PDFg		**63**	**95.2**	**0.35 ± 0.01**	**1142 ± 15**	**2.20 ± 0.08**	**0.07 ± 0.003**	**0.38 ± 0.1**

Table S3: List of fly strains.

Genotype	Reference/Source	Stock number
CLK856-Gal4	(Gummadova et al., 2009); Bloomington Drosophila Stock Center	BDSC 93198
UAS-eGFP	Bloomington Drosophila Stock Center	BDSC 5430
UAS-mRFP	Bloomington Drosophila Stock Center	BDSC 32219
UAS-Cas9.P2 (attP40)	Bloomington Drosophila Stock Center	BDSC 58985
UAS-Cas9.P2 (attP2)	Bloomington Drosophila Stock Center	BDSC 58986
AGES	(McClure et al., 2022); Bloomington Drosophila Stock Center	BDSC 92470
hsFLPG5	Bloomington Drosophila Stock Center	BDSC 55814
cry^{01}	(Dolezelova et al., 2007)	NA
PDF-Gal4	(Renn et al., 1999)	NA
CLK4.1-Gal4	(L. Zhang et al., 2010; Y. Zhang et al., 2010)	NA
dvPDF-Gal4	(Bahn et al., 2009)	NA
MB122B-Gal4	(Bulthuis et al., 2019)	Lines made by Drs. Dione, Nern and Rubin, Janelia Research Campus
ss00681-Gal4	(Liang et al., 2017)	
ss00645-Gal4	(Schlichting et al., 2019)	
ss00639-Gal4	NA	
ss00773-Gal4	NA	
UAS-STOP-Cas9 (UAS-FRT-mEGFP-FRT-uM-Cas9)	(Port et al., 2020); Vienna Drosophila Resource Center	VDRC 340008
UAS-*per-g*	(Schlichting et al., 2019)	NA
UAS-3X-vrig (attP2)	This study	NA
UAS-3X-cryg (attP2)	This study	NA
UAS-3X-Pdfg (attP2)	This study	NA

Table S4: Primer sequences used for cloning.

name	sequence 5'-> 3'
vri-1	GGCCCGGGTTCGATTCCCGGCCGATGCA**TACAGCCAGCAGAAGCTGAG**GTTTCAGAGCTATGCTGGAAAC
vri-2	**ACTGCGGTCCATTGCCACCC**TGCACCAGCCGGGAATCGAACC
vri-3	**GGGTGGCAATGGACCGCAGT**GTTTCAGAGCTATGCTGGAAAC
vri-4	TTTAACTTGCTATTTCTAGCTCTAAAAC**GACATTGCGGTTTAGTGCCT**TGCACCAGCCGGGAATCGAACC
cry-1	GGCCCGGGTTCGATTCCCGGCCGATGCA**CGCGAGGGGCGAATGTGATT**GTTTCAGAGCTATGCTGGAAAC
cry-2	**CCTGTAGCTGATCATCGATG**TGCACCAGCCGGGAATCGAACC
cry-3	**CATCGATGATCAGCTACAGG**GTTTCAGAGCTATGCTGGAAAC
cry-4	TTTAACTTGCTATTTCTAGCTCTAAAAC**TACACATTGAAGTGCTCCGG**TGCACCAGCCGGGAATCGAACC
Pdf-1	GGCCCGGGTTCGATTCCCGGCCGATGCA**TGCTGCCAGTGGGGATACTG**GTTTCAGAGCTATGCTGGAAAC
Pdf-2	**CGTTGTTGAACCAGTCGAGG**TGCACCAGCCGGGAATCGAACC
Pdf-3	**CCTCGACTGGTTCAACAACG**GTTTCAGAGCTATGCTGGAAAC
Pdf-4	TTTAACTTGCTATTTCTAGCTCTAAAAC**GCATCGTTCATGTTCTTGGG**TGCACCAGCCGGGAATCGAACC

Legend for Supplementary Dataset 1: File contains source data and statistical test for all figures.

SI References

Bahn JH, Lee G, Park JH. 2009. Comparative Analysis of Pdf-Mediated Circadian Behaviors Between Drosophila melanogaster and D. virilis. *Genetics* **181**:965–975. doi:10.1534/genetics.108.099069

Bulthuis N, Spontak KR, Kleeman B, Cavanaugh DJ. 2019. Neuronal Activity in Non-LNv Clock Cells is Required to Produce Free-Running Rest:Activity Rhythms in Drosophila. *J Biol Rhythms* **34**:249–271. doi:10.1177/0748730419841468

Dolezelova E, Dolezel D, Hall JC. 2007. Rhythm Defects Caused by Newly Engineered Null Mutations in Drosophila's cryptochrome Gene. *Genetics* **177**:329–345. doi:10.1534/genetics.107.076513

Donelson N, Kim EZ, Slawson JB, Vecsey CG, Huber R, Griffith LC. 2012. High-Resolution Positional Tracking for Long-Term Analysis of Drosophila Sleep and Locomotion Using the "Tracker" Program. *PLOS ONE* **7**:e37250. doi:10.1371/journal.pone.0037250

Emery P, So WV, Kaneko M, Hall JC, Rosbash M. 1998. CRY, a Drosophila Clock and Light-Regulated Cryptochrome, Is a Major Contributor to Circadian Rhythm Resetting and Photosensitivity. *Cell* **95**:669–679. doi:10.1016/S0092-8674(00)81637-2

Glossop NRJ, Houl JH, Zheng H, Ng FS, Dudek SM, Hardin PE. 2003. VRILLE feeds back to control circadian transcription of Clock in the Drosophila circadian oscillator. *Neuron* **37**:249–261. doi:10.1016/s0896-6273(03)00002-3

Gratz SJ, Ukken FP, Rubinstein CD, Thiede G, Donohue LK, Cummings AM, O'Connor-Giles KM. 2014. Highly specific and efficient CRISPR/Cas9-catalyzed homology-directed repair in Drosophila. *Genetics* **196**:961–971. doi:10.1534/genetics.113.160713

Gummadova JO, Coutts GA, Glossop NRJ. 2009. Analysis of the Drosophila Clock Promoter Reveals Heterogeneity in Expression between Subgroups of Central Oscillator Cells and Identifies a Novel Enhancer Region. *J Biol Rhythms* **24**:353–367. doi:10.1177/0748730409343890

Liang X, Holy TE, Taghert PH. 2017. A Series of Suppressive Signals within the Drosophila Circadian Neural Circuit Generates Sequential Daily Outputs. *Neuron* **94**:1173-1189.e4. doi:10.1016/j.neuron.2017.05.007

Ma D, Przybylski D, Abruzzi KC, Schlichting M, Li Q, Long X, Rosbash M. 2021. A transcriptomic taxonomy of Drosophila circadian neurons around the clock. *eLife* **10**:e63056. doi:10.7554/eLife.63056

McClure CD, Hassan A, Aughey GN, Butt K, Estacio-Gómez A, Duggal A, Ying Sia C, Barber AF, Southall TD. 2022. An auxin-inducible, GAL4-compatible, gene expression system for Drosophila. *eLife* **11**:e67598. doi:10.7554/eLife.67598
Port F, Bullock SL. 2016. Augmenting CRISPR applications in Drosophila with tRNA-flanked sgRNAs. *Nat Methods* **13**:852–854. doi:10.1038/nmeth.3972

Port F, Strein C, Stricker M, Rauscher B, Heigwer F, Zhou J, Beyersdörffer C, Frei J, Hess A, Kern K, Lange L, Langner N, Malamud R, Pavlović B, Rädecke K, Schmitt L, Voos L, Valentini E, Boutros M. 2020. A large-scale resource for tissue-specific CRISPR mutagenesis in Drosophila. *eLife* **9**:e53865. doi:10.7554/eLife.53865

Renn SC, Park JH, Rosbash M, Hall JC, Taghert PH. 1999. A pdf neuropeptide gene mutation and ablation of PDF neurons each cause severe abnormalities of behavioral circadian rhythms in Drosophila. *Cell* **99**:791–802. doi:10.1016/s0092-8674(00)81676-1

Schindelin J, Arganda-Carreras I, Frise E, Kaynig V, Longair M, Pietzsch T, Preibisch S, Rueden C, Saalfeld S, Schmid B, Tinevez J-Y, White DJ, Hartenstein V, Eliceiri K, Tomancak P, Cardona A. 2012. Fiji: an open-source platform for biological-image analysis. *Nat Methods* **9**:676–682. doi:10.1038/nmeth.2019

Schlichting M, Díaz MM, Xin J, Rosbash M. 2019. Neuron-specific knockouts indicate the importance of network communication to Drosophila rhythmicity. *eLife* **8**:e48301. doi:10.7554/eLife.48301

Spitzer M, Wildenhain J, Rappsilber J, Tyers M. 2014. BoxPlotR: a web tool for generation of box plots. *Nat Methods* **11**:121–122. doi:10.1038/nmeth.2811

Wiggin TD, Goodwin PR, Donelson NC, Liu C, Trinh K, Sanyal S, Griffith LC. 2020. Covert sleep-related biological processes are revealed by probabilistic analysis in Drosophila. *Proc Natl Acad Sci U S A* **117**:10024–10034. doi:10.1073/pnas.1917573117

Yoshii T, Todo T, Wülbeck C, Stanewsky R, Helfrich-Förster C. 2008. Cryptochrome is present in the compound eyes and a subset of Drosophila's clock neurons. *J Comp Neurol* **508**:952–966. doi:10.1002/cne.21702

Zhang L, Chung BY, Lear BC, Kilman VL, Liu Y, Mahesh G, Meissner R-A, Hardin PE, Allada R. 2010. DN1p Circadian Neurons Coordinate Acute Light and PDF Inputs to Produce Robust Daily Behavior in Drosophila. *Curr Biol* **20**:591–599. doi:10.1016/j.cub.2010.02.056

Zhang Y, Liu Y, Bilodeau-Wentworth D, Hardin PE, Emery P. 2010. Light and Temperature Control the Contribution of Specific DN1 Neurons to Drosophila Circadian Behavior. *Curr Biol CB* **20**:600–605. doi:10.1016/j.cub.2010.02.044